Decomposition and Equilibrium Achieving Distribution Locational Marginal Prices using Trust-Region Method

Sarmad Hanif, Student Member, IEEE, Kai Zhang, Student Member, IEEE, Christoph Hackl, Senior Member, IEEE, Masoud Barati, Senior Member, IEEE, Hoay Beng Gooi Senior Member, IEEE, Thomas Hamacher.

Abstract—We propose a new distribution locational marginal price (DLMP) model which is based on a linearized variant of the global energy balance formulation along with trust-region based solution methodology. Compared to existing DLMP works in the literature, the proposed DLMP model has shown to depict the following features: i) It decomposes into most general components, i.e., energy, loss, congestion and voltage; ii) it presents market equilibrium conditions; and ii) it is capable of achieving an efficient flexibility resource allocation in local dayahead distribution grid markets. The developed model is tested first on a benchmark IEEE 33-bus distribution grid and then on much larger grids with the inclusion of dispatch from flexible loads (FLs) and distributed generators (DGs).

Index Terms—Distribution Locational Marginal Prices (DLMPs), Linearization, Market Equilibrium, Trust-Region, Distributed Generators (DGs), Flexible Loads (FLs)

I. INTRODUCTION

The idea of establishing DLMPs has started to gain attention in the power system community [1]–[3]. Essentially, DLMPs are distribution grid variants of locational marginal prices (LMPs) at the transmission grid level [4] which provide the theoretical foundation to form deregulated energy markets around the world. As contemporary power systems are increasingly facing the integration of DGs and FLs at distribution grids, transmission level (wholesale) markets might not be sufficient for achieving economic operation in power systems. As reported in [2], [5]-[9], if not controlled properly, DGs and FLs cause congestion and higher losses in distribution grid operation. As a remedy, DLMPs are proposed as the mechanism to provide economical price signals in distribution grids, with applications ranging from loss reduction [2], [10], higher local DGs and FLs utilization [1], [10] to congestion management in distribution grids [5]-[8]. One of the major challenges, which is also the main focus of this paper is the calculation of DLMPs, that not only achieves overall grid social welfare maximization but also for local flexibility resources, with consideration of nonlinear distribution grid power flows and inter-temporal energy requirements.

A. Related Work

Almost all recent literature on DLMPs [1]–[3], [5]–[8], [10] makes the distribution service operator (DSO) responsible for running the local market with aim of maximizing the social welfare of its underlying grid. On the other hand, flexibility resources (FLs and DGs) maximize their individual surplus. The coordination between FLs/DGs and the DSO is then

This work was financially supported by the Singapore National Research Foundation under its Campus for Research Excellence And Technological Enterprise (CREATE) programme.

established to find DLMPs, maximizing the individual as well as the overall surplus of the grid, i.e. a unique dispatch for FLs and DGs. Based on the formulation of DLMPs, two broad methods, (i) lossless-DLMPs and (ii) lossy-DLMPs exist.

Recent lossless-DLMP formulations are reported in [5]–[8]. These works presented solution uniqueness and market equilibrium conditions for lossless-DLMPs with intertemporal energy requirements from FLs and DGs. However, lossless (DC) power flow formulation is used to represent distribution grids. As high resistive/impedance ratios exist in distribution grids, losses must also be considered in the proven market equilibrium conditions of lossless-DLMPs in [5]–[8].

As lossy-DLMPs are based on non-linear power flows to compute DLMPs, they are naturally more accurate in terms of representing grid conditions as compared to lossless-DLMPs. Recent works have considered linearized [10], [11], convexified [3], [12], and global power balance [1], [3], [13] variations of AC power flows to compute lossy-DLMPs. The linearized lossy-DLMP methods [10], [11] approximate AC power flows around a flat (1 p.u.) voltage magnitude across the distribution grid. Naturally, this inflicts errors in DLMPs at nodes farther away from the root-node, where a large voltage drop might occur. The convexified lossy-DLMP methods [3], [12] are more accurate than linearized AC power flows, however it does not translate to intuitive DLMP formulations [3]. This is important since the DSO must be able to interpret DLMPs and translate it into its financial settlements with market participants. The lossy-DLMPs in a most generic form are obtained from the global power balance formulation [1], [3], [13], allowing individual components of lossy-DLMPs to be analyzed in detail, which may help in interpreting DLMPs for distribution grids in a manner similar to the standardized LMP formulation of transmission grids [4]. However for DLMPs, the challenge in this formulation lies in expressing power flows which have higher nonlinearities in distribution grids as compared to those of transmission grids [3].

Another important feature of transmission grid energy markets is that the final LMP value is represented as the sum of its energy, loss and (line flow) congestion components. However, from the above mentioned lossy-DLMP formulations, only [3], [10], [11], [13] explicitly represent DLMP as the sum of its energy, loss and congestion component. Nevertheless, works in [3], [13] do not provide tractable formulation for nonlinear power flows and works in [10], [11] use static approximations (around 1 p.u. voltage) which may inflict errors in DLMP values. Hence, there exists a need to develop a DLMP model which expresses DLMP at the node as components of its energy, system loss and congestion contribution to the grid along with sufficient accuracy of nonlinear power flows.

In contrast to market equilibrium studies on lossless-

DLMPs, investigations on lossy-DLMPs have mostly focused on incorporating nonlinearities in DLMPs and have not discussed market equilibrium conditions under the presence of both instantaneous and planned time horizon flexible resource dispatch. This is important as flexibility resources (instantaneous and planned horizon dispatch) are envisioned to be an integral part of future grids and there must exist local distribution grid markets which is economically efficient, i.e., maximizing the overall grid surplus as well as the surplus of individual flexible resources.

B. Technical Contribution

In this paper, we present a tractable calculation methodology of DLMPs using a classic global power balance formulation [1], [3], [13] accounting for non-linear power flows along with multi-period dispatch from FLs and DGs operation. To tackle nonlinearities of power flows, we build upon the recent works on AC power flow approximation for distribution grids [14] and extend it to include two key components relevant for DLMPs, i.e., line flows and system losses. We deploy a trust-region based solution methodology [15] which iteratively solves convex subproblems of the overall global power balance formulation. Particular for DLMPs, these convex subproblems have two favorable properties. First, a high solution robustness is achieved as many off-the-shelf solvers exist to solve convex programs efficiently. Second, convex subproblems contain sensitivities which are directly deployed in calculating and interpreting DLMPs. Through optimality conditions, we then show that the presented DLMP formulation: i) is decomposable into energy, congestion, loss and voltage components and exists in equilibrium with grid conditions and ii) under the assumption of rational flexible resources (maximizing their individual surplus), is able to form a day-ahead local distribution grid market which achieves efficient resource allocation. In this way, we propose a method which provides a generic DLMP formulation with tractable solution methodology, beneficial for the ongoing discussions on future distribution grid markets.

Sec. II and III respectively present the system model and problem statement of this paper. The proposed methodology for calculating DLMPs along with its market equilibrium existence and flexibility resource allocation is presented in Sec. IV. The simulation setup and results follow in Sec. V.

Nomenclature

Only the most fundamental variables are mentioned here as other variables in the text are their derivatives.

```
\mathbb{N}, \mathbb{R}, \mathbb{C}
                                              sets of natural, real, complex numbers
 n,m\in \mathbb{N}
                                              grid nodes (excluding root-node), grid lines
 N\in\mathbb{N}
                                              all nodes (including root-node) N := n + 1,
 n_t \in \mathbb{N}
                                              time steps planning horizon, \mathcal{T} = \{1, \dots, n_t\}
 \underline{\mathbf{Y}} \in \mathbb{C}^{N \times N}
                                              nodal admittance matrix of the grid
 \underline{\mathbf{v}}_t \in \mathbb{C}^{\mathbb{N}}
                                              complex voltage vector (\underline{\mathbf{v}}_t = \overline{\mathbf{v}}_t \mathbf{e}^{joldsymbol{	heta}_t})
\begin{array}{l} \underline{\mathbf{v}}_t \in \mathbb{C}^{\mathbb{N}} \\ \mathbf{v}_t \in \mathbb{R}^{\mathbb{N}} \\ \boldsymbol{\theta}_t \in \mathbb{R}^{\mathbb{N}} \\ \underline{\mathbf{s}}_t \in \mathbb{C}^{\mathbb{N}} \\ \underline{\mathbf{s}}_t^{f/t} \in \mathbb{C}^{\mathrm{m}} \\ \underline{\mathbf{s}}_t^{f/t} \in \mathbb{C}^{\mathrm{m}} \\ \underline{\mathbf{p}}_t^{d/t} \mathbf{q}_t^{cl} \in \mathbb{R}^{\mathrm{n}} \\ \mathbf{p}_t^{d/t} \mathbf{q}_t^{d} \in \mathbb{R}^{\mathrm{n}} \\ \mathbf{p}_t^{h/t} \mathbf{q}_t^{d} \in \mathbb{R}^{\mathrm{n}} \\ \mathbf{ch}_t \in \mathbb{R}^{\mathrm{n}} \\ \mathbf{D}_t \in \mathbb{R}^{\mathrm{n} \times \mathrm{n}} \end{array}
                                              voltage magnitude vector
                                              voltage angle vector
                                              complex power injection vector
                                              complex line flow vector from/to nodes
                                              total complex grid losses
                                              active/reactive power of Constant Loads (CLs)
                                              active/reactive power of DGs
                                              active/reactive power of FLs
                                              state of charge FLs
 \mathbf{D}_t \in \mathbb{R}^{\bar{n} \times n}
                                              time-coupled drain matrix of FLs
\mathbf{z}_t \in \mathbb{R}^n
                                              disturbance experienced by FLs
 \mathbf{C}_t^x(\mathbf{y}_t^x) \in \mathbb{R}^n
                                             cost function for \mathbf{y}_t^x \in \{\mathbf{p}_t^x, \mathbf{q}_t^x\} with x \in \{\mathbf{g}, \mathbf{f}\} where \mathbf{g} \in \{0, \mathbf{dg}\} and 0 as the root-node supply
```

 $\Pi^{\text{Grid}}_{\mathbf{p}_t/\mathbf{q}_t} \in \mathbb{R}^n$ grid cleared active/reactive power DLMP where $[\cdot]_t$ means the value at time step t. Scalars (x) are lower case; vectors (\mathbf{x}) are bold and lower case; matrices are bold and upper case (\mathbf{X}) . Complex quantities are underlined $(\underline{\mathbf{Y}})$ with $\Re(\underline{\mathbf{Y}})$ being its real and $\Im(\underline{\mathbf{Y}})$ as its imaginary part, respectively; $\underline{\mathbf{Y}}^*$ is the complex conjugate of $\underline{\mathbf{Y}}$. Matrix $(\mathbf{X})_n$ correspondingly selects n rows and columns from \mathbf{X} ; vector $\mathbf{x}_n \in \mathbb{R}^n$ and matrix $\mathbf{X}_{n \times n} \in \mathbb{R}^{n \times n}$ contain scalar x at all entries; $\operatorname{diag}(\mathbf{x})$ turns vector \mathbf{x} to a matrix with \mathbf{x} at its diagonal; \mathbf{I}_n is the identity matrix of size n; the approximated and actual value of \mathbf{x} is given by $\tilde{\mathbf{x}}$ and $\hat{\mathbf{x}}$, respectively.

II. SYSTEM MODEL

Similar to the works on approximate distribution grid solution [14], [16] and lossy DLMP analysis [3], [10]–[13], we consider a portion of symmetric and balanced distribution grid, operating radially with n nodes plus one connection (root-node) to the transmission grid. We consider the grid to be containing constant loads (CLs) and flexibility resources (FLs and DGs) of size n. However, the developed model is naturally extendable to contain an arbitrary number of CLs, FLs and DGs. The active/reactive powers of CLs $\mathbf{p}_t^{\text{cl}}/\mathbf{q}_t^{\text{cl}} := (p_{1,t}^{\text{cl}},\dots,p_{n,t}^{\text{cl}})^{\mathsf{T}}/(q_{1,t}^{\text{cl}},\dots,q_{n,t}^{\text{cl}})^{\mathsf{T}}$ are assumed to be fixed, always satisfied by the DSO and not optimized.

A. Flexibility Resources

To show the diversity of the system model, we consider FLs planning over a time (t) horizon $\forall t \in \mathcal{T}$ and DGs dispatching instantaneous power.

The FLs are assumed to optimize their energy procurement cost of active powers for all $t \in \mathcal{T}$, i.e., $\mathbf{p}_{1}^{\mathrm{fl}} := (p_{1,t}^{\mathrm{fl}}, \dots, p_{n,t}^{\mathrm{fl}})^{\mathsf{T}}$ while keeping track of their state-of-charge (SOC) $\mathbf{ch}_{t} := (ch_{1,t}, \dots, ch_{n,t})^{\mathsf{T}}$, given an initial SOC \mathbf{ch}_{0} before the beginning of planning horizon. See (9j) for the reference. As controlling reactive power $\mathbf{q}_{t}^{\mathrm{fl}} := (q_{1,t}^{\mathrm{fl}}, \dots, q_{n,t}^{\mathrm{fl}})^{\mathsf{T}}$ is not a usual load behavior, it is kept as uncontrollable and modeled simply through a specified power factor. Note that matrix \mathbf{D}_{t} introduces coupling between time steps and can be obtained to be expressed in a form given in (9j), using the models given in [7] for electric vehicles and in [5] for air-conditioners.

The DGs are assumed to optimize their instantaneous active powers $\mathbf{p}_t^{\mathrm{dg}} := (p_{1,t}^{\mathrm{dg}}, \dots, p_{n,t}^{\mathrm{dg}})^{\mathsf{T}}$ and reactive powers $\mathbf{q}_t^{\mathrm{dg}} :=$

 $(q_{1,t}^{\mathrm{dg}},\ldots,q_{n,t}^{\mathrm{dg}})^{\mathsf{T}}$ independently. Aggregation of low voltage PV systems with controllable active and reactive power support to the grid can be considered as a practical application of these types of DGs [10].

In the framework adopted in this paper, it is assumed that DGs and FLs are price-taking, utility maximizing agents. To this end, the overall social welfare $w_{p,t}(\mathbf{p}_t^{\text{fl}}, \mathbf{p}_t^{\text{g}})$ as the aggregate benefit of DGs and FLs from the active power procurement over the planning horizon \mathcal{T} is:

$$w_{p,t}(\mathbf{p}_t^{\text{fl}}, \mathbf{p}_t^{\text{g}}) = \sum_{t=1}^{n_t} \left(\mathbf{U}_t^{\text{fl}}(\mathbf{p}_t^{\text{fl}}) - \mathbf{C}_t^{\text{g}}(\mathbf{p}_t^{\text{g}}) \right), \tag{1}$$

where $\mathbf{p}_t^{\mathrm{g}} := (p_t^0, (\mathbf{p}_t^{\mathrm{dg}})^{\mathsf{T}})^{\mathsf{T}}$ collects all individual DGs $\mathbf{p}_t^{\mathrm{dg}}$ and the root-node p_t^0 with their marginal cost of supplying energy as $\mathbf{C}_t^{\mathrm{g}}(\mathbf{p}_t^{\mathrm{g}})$. The utility function of FLs is simply the marginal cost of purchasing energy, i.e., $\mathbf{U}_t^{\mathrm{fl}}(\mathbf{p}_t^{\mathrm{fl}}) := -\mathbf{C}_t^{\mathrm{fl}}(\mathbf{p}_t^{\mathrm{fl}})$. See Sec. VII-A for the assumed cost/utility interpretations and Def. 1 for their structure. We also consider reactive power costs in the model on the basis that reactive power pricing has been the subject of interest [1], [17], [18]. As only DGs optimize their reactive power dispatch, social welfare from reactive power procurement is:

$$w_{q,t}(\mathbf{q}_t^g) = -\sum_{t=1}^{n_t} \mathbf{C}_t^g(\mathbf{q}_t^g), \tag{2}$$

with total reactive power generations: $\mathbf{q}_t^{\mathrm{g}} := (q_t^0, (\mathbf{q}_t^{\mathrm{dg}})^{\mathsf{T}})^{\mathsf{T}}$.

Definition 1: For all $x \in \{g, fl\}$ procuring power $y \in \{p, q\}$, costs are defined as $\mathbf{C}_t^x(\mathbf{y}_t^x) := \mathbf{c}_{y,t}^x ^{\mathsf{T}} \cdot \mathbf{y}_t^x$, where marginal cost is of the form $\mathbf{c}_{y,t}^x := \mathbf{a}_{y,t}^x + \mathbf{B}_{y,t}^x \mathbf{y}_t^x$ with a positive price per unit vector $\mathbf{a}_{y,t}^x \in \mathbb{R}^n$ (in \$/MWh) and symmetric, positive definite matrix $\mathbf{B}_{y,t}^x \in \mathbb{R}^{n \times n}$ of small positive price sensitivity coefficients (in \$/MWh^2), turning the social welfares introduced in (1) and (2) strictly convex.

B. Grid Model with Implicit Specification Vector

At time step t, let $\mathbf{p}_t^{\mathrm{L}} := \mathbf{p}_t^{\mathrm{dg}} - \mathbf{p}_t^{\mathrm{fl}} - \mathbf{p}_t^{\mathrm{cl}}$ & $\mathbf{q}_t^{\mathrm{L}} := \mathbf{q}_t^{\mathrm{dg}} - \mathbf{q}_t^{\mathrm{fl}} - \mathbf{q}_t^{\mathrm{cl}}$ collect active and reactive power injections. Then for $\mathbf{g}_t^{\mathrm{L}} := \mathbf{p}_t^{\mathrm{L}} + j\mathbf{q}_t^{\mathrm{L}}$ complex injections, we have $\mathbf{g}_t := (p_t^0 + jq_t^0, (\mathbf{g}_t^{\mathrm{L}})^{\mathsf{T}})^{\mathsf{T}} \in \mathbb{C}^{\mathrm{N}}$ complex injections for the whole grid. We assume a constant PQ model for these n nodes, as it's referred quite often in both classic [16] and recent distribution system studies [3], [10], [14]. In principle, the PQ model means that injections at nodes are imposed and not dependent on node voltages [14]^1. Hence, for $\mathbf{v}_t := (\underline{v}_t^0, (\mathbf{v}_t^{\mathrm{L}})^{\mathsf{T}})^{\mathsf{T}}$ collecting the whole grid complex voltages, with $\mathbf{v}_t^{\mathrm{L}} := (\underline{v}_{1,t}, \dots, \underline{v}_{n,t})^{\mathsf{T}}$ and \underline{v}_t^0 are the voltages for the n nodes and the root-node, we have the following relationship:

$$\underline{\mathbf{s}}_t = \operatorname{diag}(\underline{\mathbf{v}}_t) \underline{\mathbf{Y}}^* \underline{\mathbf{v}}_t^* \in \mathbb{C}^{\mathrm{N}}, \tag{3}$$

where matrix $\mathbf{Y} \in \mathbb{C}^{N \times N}$ is the nodal admittance matrix of the grid [14]. Under certain conditions, solving (3) for the voltages $\underline{\mathbf{v}}_t$ is called a "power flow" problem.

Relevant for radial distribution grids, the specified conditions for solving (3) exists in the form of fixing both the voltage magnitude and angle at the root-node and injections at all

¹Note that DGs providing voltage support are operated using a droop control. This droop is modeled as a response between local voltages and injected/absorbed reactive power, allowing voltage control actions to be treated as PQ buses [19, ch. 3].

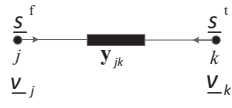


Fig. 1. For two nodes, from/to line flows definition follows: $\underline{v}^f/\underline{v}^t := \underline{v}_j/\underline{v}_k$, $\underline{\mathbf{y}}^f/\underline{\mathbf{y}}^t := (\underline{y}_{jk}, -\underline{y}_{jk})/(-\underline{y}_{jk}, \underline{y}_{jk})$ and $\underline{\mathbf{v}} := (\underline{v}_j, \underline{v}_k)^\intercal$ [21]. Similarly, these definitions can be extended to obtain $\mathbf{Y}^{f/t} \in \mathbb{C}^{m \times N}$ and $\mathbf{v}^{f/t} \in \mathbb{C}^m$.

nodes except the root-node, i.e. $\mathbf{x}_t^{\text{ref}} := (v_t^0, \theta_t^0, (\mathbf{s}_t^{\text{L}})^\intercal)^\intercal \in \mathbb{R}^{2\text{N}}$, where $\mathbf{s}_t^{\text{L}} := ((\mathbf{p}_t^{\text{L}})^\intercal, (\mathbf{q}_t^{\text{L}})^\intercal)^\intercal \in \mathbb{R}^{2\text{n}}$. Now, to solve (3) for the specified $\mathbf{x}_t^{\text{ref}}$, we introduce the manifold

$$\mathcal{M} := \left\{ \mathbf{x}_t \in \mathbb{R}^{4N} \mid \mathbf{f}(\mathbf{x}_t) = \mathbf{0}_{2N} \land \mathbf{g}(\mathbf{x}_t) = \mathbf{0}_{2N} \right\}$$
(4)

which implicitly represents the power flow problem [20], where (i) $\mathbf{x}_t := (\mathbf{v}_t^\mathsf{T}, \boldsymbol{\theta}_t^\mathsf{T}, \mathbf{p}_t^\mathsf{T}, \mathbf{q}_t^\mathsf{T})^\mathsf{T} \in \mathbb{R}^{4N}$ is the grid state vector (comprising the voltage magnitude, voltage angle, active and reactive power vector, respectively), (ii) the function

$$\mathbf{f} : \mathbb{R}^{4N} \to \mathbb{R}^{2N}, \ \mathbf{x}_t \mapsto \mathbf{f}(\mathbf{x}_t) := \begin{pmatrix} \Re\{\operatorname{diag}(\underline{\mathbf{v}}_t)\underline{\mathbf{Y}}^*\underline{\mathbf{v}}_t^* - \underline{\mathbf{s}}_t\} \\ \Im\{\operatorname{diag}(\underline{\mathbf{v}}_t)\underline{\mathbf{Y}}^*\underline{\mathbf{v}}_t^* - \underline{\mathbf{s}}_t\} \end{pmatrix}$$
(5)

expresses active power, i.e., $\mathbf{p}_t = \Re(\underline{\mathbf{s}}_t)$ and reactive power, i.e., $\mathbf{q}_t = \Im(\underline{\mathbf{s}}_t)$ from (3) and (iii) the grid model

$$\mathbf{g} \colon \mathbb{R}^{4N} \to \mathbb{R}^{2N}, \ \mathbf{x}_t \mapsto \mathbf{g}(\mathbf{x}_t) := \mathbf{g}(\mathbf{x}_t) - \mathbf{x}_t^{\text{ref}} = \mathbf{0}_{2N}$$
 (6)

considers the grid specification vector $\mathbf{x}_t^{\text{ref}}$. Let $\hat{\mathbf{v}}_t$ be the solution of (4), then for m grid lines, we have line flow vector $\mathbf{s}_t^{\text{f/t}}$ from/to the nodes (Fig. 1) and the complex grid losses, respectively, given by

$$\underline{\mathbf{s}}_{t}^{f/t} = \operatorname{diag}(\underline{\hat{\mathbf{v}}}_{t}^{f/t})\underline{\mathbf{Y}}^{f/t*}\underline{\hat{\mathbf{v}}}_{t}^{*} \in \mathbb{C}^{m}, \tag{7}$$

$$p_t^1 + jq_t^1 = s_t^1 = \hat{\mathbf{v}}_t^{\mathsf{T}} \mathbf{Y}^* \hat{\mathbf{v}}_t^* \in \mathbb{C}. \tag{8}$$

Remark 1: As classic marginal pricing [4] contains power flows as congestion components, we also opt for them. However, an extension of this model to consider thermal limits (in Amperage) can also be performed, as shown in [20, Appendix].

III. PROBLEM STATEMENT

The DSO solves the following multi-period constrained social welfare maximization problem

$$\max \quad w_t(\mathbf{p}_t^{\text{fl}}, \mathbf{p}_t^{\text{g}}, \mathbf{q}_t^{\text{g}}) := w_{p,t}(\mathbf{p}_t^{\text{fl}}, \mathbf{p}_t^{\text{g}}) + w_{q,t}(\mathbf{q}_t^{\text{g}})$$
(9a)

s.t.
$$\mathbf{1}_{\mathbf{N}}^{\mathsf{T}} \mathbf{p}_{t}^{\mathsf{g}} - \mathbf{1}_{\mathbf{n}}^{\mathsf{T}} (\mathbf{p}_{t}^{\mathsf{cl}} + \mathbf{p}_{t}^{\mathsf{fl}}) = p_{t}^{\mathsf{l}} : \lambda_{t}^{p}$$
 (9b)

$$\mathbf{1}_{\mathbf{N}}^{\top} \mathbf{q}_{t}^{\mathbf{g}} - \mathbf{1}_{\mathbf{n}}^{\top} (\mathbf{q}_{t}^{\mathbf{cl}} + \mathbf{q}_{t}^{\mathbf{fl}}) = q_{t}^{\mathbf{l}} \qquad : \lambda_{t}^{q}$$
 (9c)

$$|\underline{\mathbf{s}}_t^{\mathrm{f}}|^2 \le (\mathbf{s}_t^{\mathrm{f+}})^2 \qquad \qquad : \boldsymbol{\mu}_{s_t^{\mathrm{f}}}^+ \qquad \qquad (9\mathrm{d})$$

$$|\underline{\mathbf{s}}_t^{\mathsf{t}}|^2 \le (\mathbf{s}_t^{\mathsf{t}+})^2 \qquad \qquad : \boldsymbol{\mu}_{s_t^{\mathsf{t}}}^+ \tag{9e}$$

$$\mathbf{v}_t^{L-} \le \mathbf{v}_t^L \le \mathbf{v}_t^{L+} \qquad \qquad : \boldsymbol{\mu}_{\mathbf{v}_t^L}^{-}, \boldsymbol{\mu}_{\mathbf{v}_t^L}^{+} \quad \text{(9f)}$$

$$\mathbf{p}_t^{\mathrm{dg}-} \leq \mathbf{p}_t^{\mathrm{dg}} \leq \mathbf{p}_t^{\mathrm{dg}+} \qquad \qquad : \boldsymbol{\mu}_{\mathbf{p}_t}^{\mathrm{dg}-}, \boldsymbol{\mu}_{\mathbf{p}_t}^{\mathrm{dg}+} \tag{9g}$$

$$\mathbf{q}_t^{\mathrm{dg}-} \leq \mathbf{q}_t^{\mathrm{dg}} \leq \mathbf{q}_t^{\mathrm{dg}+} \\ : \boldsymbol{\mu}_{\mathbf{q}_t}^{\mathrm{dg}-}, \boldsymbol{\mu}_{\mathbf{q}_t}^{\mathrm{dg}+} \ \ (9\mathrm{h})$$

$$\mathbf{p}_t^{\mathrm{fl}-} \le \mathbf{p}_t^{\mathrm{fl}} \le \mathbf{p}_t^{\mathrm{fl}+} \qquad \qquad : \boldsymbol{\mu}_{\mathbf{p}_t}^{\mathrm{fl}-}, \boldsymbol{\mu}_{\mathbf{p}_t}^{\mathrm{fl}+} \quad (9\mathrm{i})$$

$$\mathbf{ch}_t^{\mathrm{fl-}} \leq \mathbf{ch}_0^{\mathrm{fl}} + \mathbf{D}_t \mathbf{p}_t^{\mathrm{fl}} - \mathbf{z}_t \leq \mathbf{ch}_t^{\mathrm{fl+}} : \boldsymbol{\mu}_{\mathbf{ch}_t}^{\mathrm{fl-}}, \boldsymbol{\mu}_{\mathbf{ch}_t}^{\mathrm{fl+}}$$
(9j)

for all $t \in \mathcal{T} = \{1, \dots, n_t\}$. Constraints (9b) and (9c) respectively present global active and reactive power balance

of the distribution grid. From (8), we denote active power loss as p_t^l and reactive power loss as q_t^l . Constraint (9i) manges dispatch capabilities of FLs within the allowable inter-temporal SOC constraints (9j). All DGs' active/reactive power are constrained through (9g)/(9h), respectively. Apparent power flowing in distribution grid lines from/to ends of the lines are constrained through (9d)/(9e). The variables listed to the right of each constraint (behind colon) are their respective Lagrangian multipliers. The optimization problem in (9) is a classical global energy balance formulation for calculating DLMPs [3], [4]. However, unlike transmission grid's single period, it deploys multi-period modeling as:

- it allows for a more accurate description of flexible load modeling, because closer to the consumption (distribution grids), static aggregated load modeling of transmission grids might not be accurate [22];
- it aids in scheduling flexibility resources with intertemporal energy requirements; and
- it allows for a wide range of model applications and extensions (see Sec. IV-F).

However, a great barrier for solving (9) in its given form comes from constraints (9b)–(9f), as they are highly nonlinear and non-convex and in general not easy to represent in a closed-form tractable fashion [see (4)–(8)]. Hence, this renders the DLMP determination from (9) difficult as off-the-shelf solvers can not solve it in this form, reducing solution reliability and future practical realization of DLMPs.

IV. PROPOSED METHODOLOGY

In order to deal with the above stated barrier for solving (9), we propose to implement a linearized variant of (9) along with a trust-region update procedure. In principle, at each iteration, convex sub-problems of (9) are obtained. These convex sub-problem are then iteratively solved and checked against the actual power flow solution to guarantee feasibility and improvement in the obtained solution of convex subproblems.

A. Implicit Power Flow Linearization

We now build upon upon the work in [20] to obtain a linear approximation of the implicit power flow representation (4) and extend it for the relevant DLMP calculations.

From [20, Lemma 1], (4) is actually a smooth manifold, allowing us to attach a tangent plane to every operating point $\hat{\mathbf{x}}_t$ in (4). Hence, for a given input $\mathbf{x}_t^{\text{ref}}$ and state $\hat{\mathbf{x}}_t$ satisfying the nonlinear manifold (4), we have the following first order approximation for the new solution state $\tilde{\mathbf{x}}_t$:

$$\begin{pmatrix} \mathbf{f}(\tilde{\mathbf{x}}_t) \\ \mathbf{g}(\tilde{\mathbf{x}}_t) \end{pmatrix} \approx \begin{pmatrix} \mathbf{0}_{2N} \\ \mathbf{x}_t^{\text{ref}} \end{pmatrix} + \begin{bmatrix} \mathbf{J}(\hat{\mathbf{x}}_t) \\ \mathbf{G} \end{bmatrix} (\tilde{\mathbf{x}}_t - \hat{\mathbf{x}}_t), \quad (10)$$

where the explicit tangent (Jacobian) matrix is

$$\mathbf{J}(\mathbf{\hat{x}}_t) = \left\lceil \left(\langle \operatorname{diag}(\underline{\mathbf{Y}}^* \mathbf{\hat{\underline{v}}}_t^*) \rangle + \langle \operatorname{diag}(\mathbf{\hat{\underline{v}}}_t) \rangle \mathbf{N} \langle \underline{\mathbf{Y}} \rangle \right) \mathbf{R}(\mathbf{\hat{\underline{v}}}_t), \ -\mathbf{I}_{2N} \right\rceil \in \mathbb{R}^{2N \times 4N}$$

represented using the following shorthands

$$\mathbf{N} := \begin{bmatrix} \mathbf{I}_N, & \mathbf{O}_{N \times N} \\ \mathbf{O}_{N \times N}, & -\mathbf{I}_N \end{bmatrix}, \ \langle \underline{\mathbf{A}} \rangle := \begin{bmatrix} \Re(\underline{\mathbf{A}}), & -\Im(\underline{\mathbf{A}}) \\ \Im(\underline{\mathbf{A}}), & \Re(\underline{\mathbf{A}}) \end{bmatrix} \in \mathbb{R}^{2N \times 2N},$$

$$\mathbf{R}(\underline{\mathbf{v}}) := \begin{bmatrix} \operatorname{diag}(\mathbf{cos}\,\boldsymbol{\theta}) & -\operatorname{diag}(\mathbf{v})\operatorname{diag}(\mathbf{sin}\,\boldsymbol{\theta}) \\ \operatorname{diag}(\mathbf{sin}\,\boldsymbol{\theta}) & \operatorname{diag}(\mathbf{v})\operatorname{diag}(\mathbf{cos}\,\boldsymbol{\theta}) \end{bmatrix} \in \mathbb{R}^{2N \times 2N}.$$

The matrix **G** selects specified entries in $\mathbf{x}_t^{\text{ref}}$ from the overall state vector \mathbf{x}_t as,

$$\mathbf{G} := \begin{bmatrix} \begin{smallmatrix} (\mathbf{1}, \mathbf{0}_{\mathbf{1}}^\mathsf{T}) & \mathbf{0}_{\mathbf{1}}^\mathsf{T} & \mathbf{0}_{\mathbf{1}}^\mathsf{T} & \mathbf{0}_{\mathbf{1}}^\mathsf{T} \\ \mathbf{0}_{\mathbf{N}}^\mathsf{T} & (\mathbf{1}, \mathbf{0}_{\mathbf{1}}^\mathsf{T}) & \mathbf{0}_{\mathbf{N}}^\mathsf{T} & \mathbf{0}_{\mathbf{1}}^\mathsf{T} \\ \mathbf{0}_{\mathbf{n} \times \mathbf{N}} & \mathbf{0}_{\mathbf{n} \times \mathbf{N}} & [\mathbf{0}_{\mathbf{n}} & \mathbf{I}_{\mathbf{n}}] & \mathbf{0}_{\mathbf{N} \times \mathbf{N}}^\mathsf{T} \\ \mathbf{0}_{\mathbf{n} \times \mathbf{N}} & \mathbf{0}_{\mathbf{n} \times \mathbf{N}} & [\mathbf{0}_{\mathbf{n}} & \mathbf{I}_{\mathbf{n}}] & \mathbf{0}_{\mathbf{n} \times \mathbf{N}}^\mathsf{T} \\ \mathbf{0}_{\mathbf{n} \times \mathbf{N}} & \mathbf{0}_{\mathbf{n} \times \mathbf{N}} & [\mathbf{0}_{\mathbf{n}} & \mathbf{I}_{\mathbf{n}}] & \mathbf{0}_{\mathbf{N} \times \mathbf{N}}^\mathsf{T} \\ \end{bmatrix} \in \mathbb{R}^{2N \times 4N}$$

For a practical radial distribution grid, the system of (10) is invertible [20], allowing us to obtain an approximate state vector $\tilde{\mathbf{x}}_t$, given an operating point $\hat{\mathbf{x}}_t$ and input $\mathbf{x}_t^{\text{ref}}$. As a result, we obtain an important matrix from $\mathbf{J}(\hat{\mathbf{x}}_t)^{-1}$, defined as:

$$\mathbf{M}_{\mathbf{p}_{t},\mathbf{q}_{t}}^{\mathbf{v}_{t},\boldsymbol{\theta}_{t}} := \begin{bmatrix} \mathbf{M}_{\mathbf{p}_{t},\mathbf{q}_{t}}^{\mathbf{v}_{t}} \\ \mathbf{M}_{\mathbf{p}_{t},\mathbf{q}_{t}}^{\boldsymbol{\theta}_{t}} \end{bmatrix} := \begin{bmatrix} \frac{\partial \hat{\mathbf{v}}_{t}}{\partial \hat{\mathbf{p}}_{t}} & \frac{\partial \hat{\mathbf{v}}_{t}}{\partial \hat{\mathbf{q}}_{t}} \\ \frac{\partial \hat{\boldsymbol{\theta}}_{t}}{\partial \hat{\boldsymbol{p}}_{t}} & \frac{\partial \hat{\boldsymbol{\theta}}_{t}}{\partial \hat{\boldsymbol{q}}_{t}} \end{bmatrix} \in \mathbb{R}^{2N \times 2N}, \quad (11)$$

providing sensitivity of power flow solution, i.e., voltage magnitude $\hat{\mathbf{v}}_t$ and angle $\hat{\boldsymbol{\theta}}_t$, given the active \mathbf{p}_t and reactive power injection \mathbf{q}_t in the grid.

B. Constraints Linearization

We seek the following approximations of non-convex parts of (9b)–(9f),

$$\tilde{\mathbf{v}}_t^{\mathrm{L}} \approx \hat{\mathbf{a}}_t + \mathbf{M}^{\mathbf{v}_t^{\mathrm{L}}} \mathbf{s}_t^{\mathrm{L}},$$
 (12a)

$$|\tilde{\mathbf{s}}_t^f|^2 \approx \hat{\mathbf{b}}_t + \mathbf{M}^{\underline{\mathbf{s}}_t^f} \mathbf{s}_t^{\text{inj}},$$
 (12b)

$$|\tilde{\mathbf{s}}_t^t|^2 \approx \hat{\mathbf{c}}_t + \mathbf{M}^{\underline{\mathbf{s}}_t^t} \mathbf{s}_t^{\mathrm{inj}},$$
 (12c)

$$\tilde{p}_t^l \approx \hat{d}_t + \mathbf{M}^{p_t^l} \mathbf{s}_t^{\text{inj}},$$
 (12d)

$$\tilde{q}_t^1 \approx \hat{e}_t + \mathbf{M}^{q_t^1} \mathbf{s}_t^{\text{inj}},$$
 (12e)

which, for given operating conditions $(\hat{\mathbf{a}}_t, \hat{\mathbf{b}}_t, \hat{\mathbf{c}}_t, \hat{d}_t, \hat{e}_t)$, are linear in the augmented active and reactive power injections vector for the whole grid $\mathbf{s}_t^{\text{inj}} := (\mathbf{p}_t^{\mathsf{T}}, \mathbf{q}_t^{\mathsf{T}})^{\mathsf{T}}$ and PQ nodes $\mathbf{s}_t^{\mathsf{L}} := (\mathbf{p}_t^{\mathsf{LT}}, \mathbf{q}_t^{\mathsf{LT}})^{\mathsf{T}}$.

- 1) Linear Voltage Magnitude: For a given operation $(\hat{\mathbf{v}}_t^L, \hat{\mathbf{s}}_t^L)$, (12a) is obtained by first directly choosing sensitivity terms from $\mathbf{M}_{\mathbf{p}_t,\mathbf{q}_t}^{\mathbf{v}_t,\theta_t}$ which corresponds to voltage magnitude, i.e., $\mathbf{M}^{\mathbf{v}_t^L} := (\mathbf{M}_{\mathbf{p}_t,\mathbf{q}_t}^{\mathbf{v}_t,\theta_t})_n$ and then setting $\hat{\mathbf{a}}_t := \hat{\mathbf{v}}_t^L \mathbf{M}_t^{\mathbf{v}_t^L} \hat{\mathbf{s}}_t^L$
- 2) Linear Squared Line Flow: For squared line flows "from" nodes expressed as $|\underline{\mathbf{s}}_t^{\mathrm{f}}|^2 := \mathrm{diag}(\underline{\mathbf{s}}_t^{\mathrm{f*}})\underline{\mathbf{s}}_t^{\mathrm{f}}$, we proceed to obtain the desired sensitivities as follows:

$$\begin{split} \mathbf{M}^{\underline{\mathbf{s}}_{t}^{\mathrm{f}}} &:= \frac{\partial |\underline{\mathbf{s}}_{t}^{\mathrm{f}}|^{2}}{\partial \mathbf{s}_{t}^{\mathrm{inj}}} = \mathrm{diag}(\underline{\mathbf{s}}^{\mathrm{f}*}) \frac{\partial \underline{\mathbf{s}}_{t}^{\mathrm{f}}}{\partial \mathbf{s}_{t}^{\mathrm{inj}}} + \mathrm{diag}(\underline{\mathbf{s}}_{t}^{\mathrm{f}}) \frac{\partial \underline{\mathbf{s}}_{t}^{\mathrm{f}*}}{\partial \mathbf{s}_{t}^{\mathrm{inj}}} \\ &= \mathrm{diag}\left(\Re(\underline{\mathbf{s}}_{t}^{\mathrm{f}}) - \Im(\underline{\mathbf{s}}_{t}^{\mathrm{f}})\right) \left(\Re(\frac{\partial \underline{\mathbf{s}}_{t}^{\mathrm{f}}}{\partial \mathbf{s}_{t}^{\mathrm{inj}}}) + \Im(\frac{\partial \underline{\mathbf{s}}_{t}^{\mathrm{f}}}{\partial \mathbf{s}_{t}^{\mathrm{inj}}})\right) \\ &+ \mathrm{diag}\left(\Re(\underline{\mathbf{s}}_{t}^{\mathrm{f}}) + \Im(\underline{\mathbf{s}}_{t}^{\mathrm{f}})\right) \left(\Re(\frac{\partial \underline{\mathbf{s}}_{t}^{\mathrm{f}}}{\partial \mathbf{s}_{t}^{\mathrm{inj}}}) - \Im(\frac{\partial \underline{\mathbf{s}}_{t}^{\mathrm{f}}}{\partial \mathbf{s}_{t}^{\mathrm{inj}}})\right), \\ &\text{with cross products canceling out to give,} \\ &= 2\bigg(\operatorname{diag}\left(\Re(\underline{\mathbf{s}}_{t}^{\mathrm{f}})\right)\Re(\frac{\partial \underline{\mathbf{s}}_{t}^{\mathrm{f}}}{\partial \mathbf{s}_{t}^{\mathrm{inj}}}) + \operatorname{diag}\left(\Im(\underline{\mathbf{s}}_{t}^{\mathrm{f}})\right)\Im(\frac{\partial \underline{\mathbf{s}}_{t}^{\mathrm{f}}}{\partial \mathbf{s}_{t}^{\mathrm{inj}}})\bigg) \\ &= 2\bigg(\operatorname{diag}\left(\Re(\underline{\mathbf{s}}_{t}^{\mathrm{f}})\right), \operatorname{diag}\left(\Im(\underline{\mathbf{s}}_{t}^{\mathrm{f}})\right)\bigg) \left[\frac{\Re(\frac{\partial \underline{\mathbf{s}}_{t}^{\mathrm{f}}}{\partial \mathbf{s}_{t}^{\mathrm{inj}}})}{\Im(\frac{\partial \underline{\mathbf{s}}_{t}^{\mathrm{f}}}{\partial \mathbf{s}_{t}^{\mathrm{inj}}})}\right]. \end{split}$$

Now, the above required sensitivities are obtained from the following chain rule:

$$\begin{bmatrix} \Re(\frac{\partial \underline{\mathbf{s}}_{t}^{l}}{\partial \mathbf{s}_{t}^{in}}) \\ \Im(\frac{\partial \underline{\mathbf{s}}_{t}^{l}}{\partial \mathbf{s}_{t}^{in}}) \end{bmatrix} = \begin{bmatrix} \Re(\frac{\partial \underline{\mathbf{s}}_{t}^{l}}{\partial \mathbf{v}_{t}} \cdot \frac{\partial \mathbf{v}_{t}}{\partial \mathbf{s}^{in}}) \\ \Im(\frac{\partial \underline{\mathbf{s}}_{t}^{l}}{\partial \underline{\mathbf{v}}_{t}} \cdot \frac{\partial \underline{\mathbf{v}}_{t}}{\partial \mathbf{s}^{in}}) \end{bmatrix} = \begin{bmatrix} \Re(\frac{\partial \underline{\mathbf{s}}_{t}^{l}}{\partial \underline{\mathbf{v}}_{t}}) \\ \Im(\frac{\partial \underline{\mathbf{s}}_{t}^{l}}{\partial \underline{\mathbf{v}}_{t}}) \end{bmatrix} \mathbf{M}_{\mathbf{p}_{t}, \mathbf{q}_{t}}^{\mathbf{v}_{t}, \boldsymbol{\theta}_{t}},$$

where the line flow sensitivities in terms of voltages are computed from (7). However, in order to utilize the approximation in (11), we compute line flow sensitivities in a from similar to (10), i.e., by replacing the injection variables $(\mathbf{p}_t, \mathbf{q}_t)$ with line flow variables $(\Re(\underline{\mathbf{s}}_t^f), \Im(\underline{\mathbf{s}}_t^f))$. Finally, we have the desired explicit tangent matrix of line flows in power injections as:

$$\begin{split} \mathbf{M}^{\underline{\mathbf{s}}_t^f} &= 2 \Big(\operatorname{diag}(\Re(\underline{\mathbf{s}}_t^f)), \operatorname{diag}(\Im(\underline{\mathbf{s}}_t^f)) \Big) \Big(\mathbf{X} + \mathbf{Y} \Big) \mathbf{M}^{\mathbf{v}_t, \boldsymbol{\theta}_t}_{\mathbf{p}_t, \mathbf{q}_t} \in \mathbb{R}^{m \times 2N}, \\ & \text{(13)} \\ \text{where } \mathbf{X} := \left\langle \operatorname{diag}(\underline{\mathbf{Y}}^f \hat{\underline{\mathbf{v}}}_t) \mathbf{A}^f \right\rangle \text{ and } \mathbf{Y} := \left\langle \operatorname{diag}(\mathbf{A}^f \hat{\mathbf{v}}_t^*) \underline{\mathbf{Y}}^f \right\rangle \text{ with incidence matrix } \mathbf{A}^f \text{ arranged such that } \mathbf{v}_t^f := \mathbf{A}^f \mathbf{v}_t. \text{ Now by setting, } \hat{\mathbf{b}}_t := |\underline{\hat{\mathbf{s}}}_t^f|^2 - \mathbf{M}^{\underline{\mathbf{s}}_t^f} \hat{\mathbf{s}}_t^{inj} \text{ we recover (12b). A similar procedure exists for (12c) and is left out here to save space. \end{split}$$

3) Linearized system losses: Similar to the above sensitivity derivation, consider the following chain rule

$$\begin{bmatrix} \mathbf{M}_t^{p^l} \\ \mathbf{M}_t^{q^l} \end{bmatrix} := \begin{bmatrix} \Re(\frac{\partial s_t^l}{\partial \mathbf{s}_{t}^{in}}) \\ \Im(\frac{\partial s_t^l}{\partial \mathbf{s}_{t}^{in}}) \end{bmatrix} = \begin{bmatrix} \Re(\frac{\partial s_t^l}{\partial \mathbf{v}_t} \cdot \frac{\partial \mathbf{v}_t}{\partial \mathbf{s}_{t}^{in}}) \\ \Im(\frac{\partial s_t^l}{\partial \mathbf{v}_t} \cdot \frac{\partial \mathbf{v}_t}{\partial \mathbf{s}_{t}^{in}}) \end{bmatrix} = \begin{bmatrix} \Re(\frac{\partial s_t^l}{\partial \mathbf{v}_t}) \\ \Im(\frac{\partial s_t^l}{\partial \mathbf{v}_t}) \end{bmatrix} \mathbf{M}_{\mathbf{p}_t, \mathbf{q}_t}^{\mathbf{v}_t, \boldsymbol{\theta}_t},$$

now using the system loss definition from (8), along with the above chain rule we get the desired system loss tangents to injections,

$$\begin{bmatrix} \mathbf{M}_{t}^{p^{l}} \\ \mathbf{M}_{t}^{q^{l}} \end{bmatrix} := \left(\langle (\underline{\mathbf{Y}} \, \hat{\underline{\mathbf{v}}}_{t})^{\mathsf{T}} \rangle + \langle \hat{\underline{\mathbf{v}}}_{t}^{\mathsf{T}} \rangle \mathbf{N} \langle \underline{\mathbf{Y}} \rangle \right) \mathbf{R}(\hat{\underline{\mathbf{v}}}_{t}) \mathbf{M}_{\mathbf{p}_{t}, \mathbf{q}_{t}}^{\mathbf{v}_{t}, \boldsymbol{\theta}_{t}} \in \mathbb{R}^{2 \times 2 \mathbf{N}}.$$
(14)

We then recover (12d) and (12e) by setting

$$\begin{bmatrix} \hat{d}_t \\ \hat{e}_t \end{bmatrix} := \begin{bmatrix} \hat{p}_t^l \\ \hat{q}_t^l \end{bmatrix} - \begin{bmatrix} \mathbf{M}^{p_t^l} \\ \mathbf{M}^{q_t^l} \end{bmatrix} \mathbf{\hat{s}}_t^{\text{inj}}.$$

C. Linearized Multi-Period Optimal Power Flow (LMOPF) with Trust Region Solution Algorithm

1) Linearized Multi-Period Optimal Power Flow (LMOPF): By replacing the non-convex parts of (9b)–(9f) in (9) with their respective linear approximates in (12), we form the LMOPF problem

$$\max \quad w_t(\tilde{\mathbf{p}}_t^{\mathrm{fl}}, \tilde{\mathbf{p}}_t^{\mathrm{g}}, \tilde{\mathbf{q}}_t^{\mathrm{g}}) := w_{p,t}(\tilde{\mathbf{p}}_t^{\mathrm{fl}}, \tilde{\mathbf{p}}_t^{\mathrm{g}}) + w_{q,t}(\tilde{\mathbf{q}}_t^{\mathrm{g}}) \qquad (15a)$$

s.t.
$$(12)$$
, $(9b) - (9j)$ $(15b)$

for all $t \in \mathcal{T} = \{1, \dots, n_t\}$. Given a dispatch $\hat{\mathbf{s}}_t^{\text{disp}} := ((\hat{\mathbf{p}}_t^g)^\intercal, (\hat{\mathbf{p}}_t^f)^\intercal, (\hat{\mathbf{q}}_t^g)^\intercal)^\intercal$ satisfying the current system state $\hat{\mathbf{x}}_t$, (15) outputs new dispatch $\tilde{\mathbf{s}}_t^{\text{disp}} := ((\tilde{\mathbf{p}}_t^g)^\intercal, (\tilde{\mathbf{p}}_t^f)^\intercal, (\tilde{\mathbf{q}}_t^g)^\intercal)^\intercal$ to maximize the overall social welfare.

Remark 2: The LMOPF in (15) is a quadratic program (QP). This is because the LMOPF has a positive definite Hessian term in the objective function (*Definition*. 1) along with constraints which are linear in the dispatch variables (Sec. IV-B).

2) Trust-region Algorithm: The trust-region methods have been applied to optimal power flow problems [23]. However, they have not yet been deployed for radial distribution grids with implicit specification vector (4), which is the focus of this paper. In this paper, we deploy trust-region based algorithm to mitigate the approximation inaccuracy from the LMOPF dispatch $\mathbf{\tilde{s}}_t^{\text{disp}}$. This is because given the operation point $\mathbf{\hat{x}}_t$, dispatch $\mathbf{\tilde{s}}_t^{\text{disp}}$ may move the approximation $\mathbf{\tilde{x}}_t$ in (10) too far from $\mathbf{\hat{x}}_t$, rendering the linearization in (12) inaccurate, i.e., not giving an accurate reflection of the original power flow (4).

Algorithm 1 describes a trust-region based methodology in 4 steps. The steps improve the approximate solution of the

Algorithm 1: Trust-Region Algorithm

```
Input Using initial dispatch quantities \hat{\mathbf{s}}_t^{\mathrm{disp}}(0) perform a base case
  power flow to obtain feasible state \hat{\mathbf{x}}_t(0) satisfying (4)
while |\Delta \tilde{\mathbf{s}}_t^{disp}(m)|_{\infty} \geq \epsilon do
       Step 1: Trust-region Minimization;
       From a feasible \hat{\mathbf{x}}_t(m), obtain (12) and solve (15) to
       get \tilde{\mathbf{s}}_t^{	ext{disp}}(m) ;
Step 2: Feasible Solution Projection ;
       Using \tilde{\mathbf{s}}_t^{\mathrm{disp}}(m) solve (4) to obtain a new feasible state \hat{\mathbf{x}}_t(m)
         and a corresponding feasible dispatch \hat{\mathbf{s}}_{t}^{\text{disp}}(m);
       Step 3: Trust Region Evaluation and Update;
                                                                   /* bad approx. */
       if \sigma(m) \leq \eta then
      \begin{array}{l} \mid \ \delta(m+1) = \gamma \cdot \delta(m); \\ \text{else if } \sigma(m) > (1-\eta) \text{ then} \\ \mid \ \delta(m+1) = \min(2\delta(m), \delta_{\max}); \end{array}
                                                                /* good approx. */
              \delta(m+1) = \delta(m);
       end
       Step 4: Evaluate Solution Progress;
       if \sigma(m) > \tau then
              Accept the iteration, set new states as \hat{\mathbf{x}}_t(m);
              Reject the iteration and repeat using the modified region;
      end
end
```

LMOPF in an iterative manner for each iteration m. First, by solving the LMOPF (QP), the minimization stage generates the steepest-decent moving step for the variables within the trust region [15]. In this step, the trust-region permissible value for variables to move is determined by radius δ , which is included in all inequality constraints of the LMOPF. Now using the dispatch result in the first step, a new operational point $\tilde{\mathbf{x}}_t(m)$ is projected to the actual power flows (4). Then the trust-region radius is evaluated for the current iteration m using the following criteria:

$$\sigma(m) = \frac{w_t(\hat{\mathbf{s}}_t^{\text{disp}}(m-1)) - w_t(\hat{\mathbf{s}}_t^{\text{disp}}(m))}{w_t(\hat{\mathbf{s}}_t^{\text{disp}}(m-1)) - w_t(\tilde{\mathbf{s}}_t^{\text{disp}}(m))}.$$
 (16)

The above definition of $\sigma(m)$ represents the ratio between the cost improvement of approximated system to the actual one. A smaller value of $\sigma(m)$ shows that the current approximation does not represent the actual system and hence the optimization region must be reduced. For a considerably higher value of $\sigma(m)$, the linear approximation is accurate and the system can move to a new operating point. As a termination criteria, when the change in two consecutive LMOPF dispatch, i.e., $|\Delta \tilde{\mathbf{s}}_t^{\text{disp}}(m)|_{\infty} := \max|\tilde{\mathbf{s}}_t^{\text{disp}}(m) - \tilde{\mathbf{s}}_t^{\text{disp}}(m-1)|$ where $|\cdot|$ is the absolute operator, is below a certain threshold ϵ , Algorithm 1 terminates. For the choice of γ , ϵ , η , τ and δ_{max} , interested readers are referred to [23].

3) Solution Uniqueness: For the implicit function representation of (4) with input $\mathbf{x}_t^{\text{ref}}$, following sufficient condition (17) exists for a unique solution for a practical grid operation, i.e. $\hat{\mathbf{v}}_t$ within usual operating range [14, Theorem 1]:

$$(v_t^0)^2 > 4l_{max}s_t,$$
 (17)

with the approximation $\tilde{\mathbf{v}}_t$ in (10) bounded by [14, Collary 2],

$$|\tilde{\mathbf{v}}_t - \hat{\mathbf{v}}_t| \le \frac{4}{(v_t^0)^3} l_i l_{max} s_t^2. \tag{18}$$

The quantities l_i , l_{max} and s_t are the impedance path to node i from root-node, maximum impedance length of the

grid and total load of the grid, respectively. Now assuming the dispatch $\hat{\mathbf{s}}_t^{\text{disp}}(m)$ at iteration m satisfies (17), then the approximated dispatch $\tilde{\mathbf{s}}_t^{\text{disp}}(m)$ from (15) is unique. This is because the LMOPF is a QP (see Remark 2). Moving on, as the Algorithm 1, through trust-region ensures that each iteration's imposed dispatch $\tilde{\mathbf{s}}_t^{\text{disp}}(m)$ satisfies grid operations from (4), it maintains the power flow uniqueness for practical operating conditions (17). Given the feasibility of (4) and the solution uniqueness (17), Algorithm 1 terminates when improvement in dispatch $\tilde{\mathbf{s}}_t^{\text{disp}}(m)$ stops, achieving a unique solution for the given trust-region valid in (4), i.e. $\tilde{\mathbf{s}}_t^{\text{disp}}(m) = \hat{\mathbf{s}}_t^{\text{disp}}(m)$.

4) Formulation/Solution Benefits: method (Algorithm 1) handles non convexity in two steps; (i) AC power flow calculations (for feasibility checking) and (ii) convex subproblems optimization (maximizing social welfare). Both these steps have off-the-shelf software packages that can handle large-sized problems. In this way, the proposed method relies on mature technology, providing high solution reliability and robustness. Moreover, approximations of (12) are already embedded in the LMOPF (15), aiding in the interpretation and calculation of DLMPs, as demonstrated next in Proposition 1 of Sec. IV-D. Note that instead of handling non-convexity in two steps (proposed model), another option could have been to formulate convexified power flow radial grid models [24]-[27]. However, we show in Sec. VII-B that the convexified formulation might not translate to an intuitive DLMP formulation and interpretation.

D. DLMPs: Decomposition & Market Equilibrium

Utilizing the solution methodology provided in the above subsection, we now derive DLMPs, satisfying market equilibrium along with decomposable in grid conditions.

Proposition 1: For active power procurement at each time step t, there exist active power DLMPs, i.e., $\Pi_{\mathbf{p}_t}^{\mathrm{Grid}}$, which are under equilibrium and completely representable for the whole grid as the sum of their (i) energy $\Pi_{\mathbf{p}_t}^{\mathrm{E}}$, (ii) loss $\Pi_{\mathbf{p}_t}^{\mathrm{L}}$, (iii) congestion $\Pi_{\mathbf{p}_t}^{\mathrm{C}}$ and (iv) voltage $\Pi_{\mathbf{p}_t}^{\mathrm{V}}$ components, i.e.,

$$\Pi_{\mathbf{p}_t}^{\text{Grid}} = \Pi_{\mathbf{p}_t}^{\text{E}} + \Pi_{\mathbf{p}_t}^{\text{L}} + \Pi_{\mathbf{p}_t}^{\text{C}} + \Pi_{\mathbf{p}_t}^{\text{V}} \in \mathbb{R}^n.$$
 (19)

 $\begin{array}{l} \text{uniquely determined as: } \boldsymbol{\Pi}_{\mathbf{p}_{t}}^{\mathbf{E}} := c_{p,t}^{0} \mathbf{1}_{\mathbf{n}}, \ \boldsymbol{\Pi}_{\mathbf{p}_{t}}^{\mathbf{L}} := \\ -(\mathbf{M}_{\mathbf{p}_{t}}^{p_{t}^{l}})_{\mathbf{n}}^{\mathsf{T}} c_{p,t}^{0} - (\mathbf{M}_{\mathbf{p}_{t}}^{q_{t}^{l}})_{\mathbf{n}}^{\mathsf{T}} c_{q,t}^{0}, \ \boldsymbol{\Pi}_{\mathbf{p}_{t}}^{\mathbf{C}} := (\mathbf{M}_{\mathbf{p}_{t}}^{\underline{\mathbf{s}}_{t}^{l}})_{\mathbf{n}}^{\mathsf{T}} \boldsymbol{\mu}_{s_{t}^{f}} + \\ (\mathbf{M}_{\mathbf{p}_{t}}^{\mathbf{v}_{t}^{l}})_{\mathbf{n}} \boldsymbol{\mu}_{s_{t}^{l}} \ \text{and } \boldsymbol{\Pi}_{\mathbf{p}_{t}}^{\mathbf{V}} := \mathbf{M}_{\mathbf{p}_{t}}^{\mathbf{v}_{t}^{l}} (\boldsymbol{\mu}_{\mathbf{v}_{t}^{l}}^{-} - \boldsymbol{\mu}_{\mathbf{v}_{t}^{l}}^{+})^{2}. \end{array}$

Proof: Consider the KKT conditions to be satisfied by

 2 Matrix $\mathbf{M}_{\mathbf{p}_t/\mathbf{q}_t}^{[\cdot]}$ corresponds to active/reactive power parts of $\mathbf{M}^{[\cdot]}$. Marginal cost of active/reactive power supply at the root-node is $c_{p,t}^0/c_{q,t}^0$.

the solution of the LMOPF problem $\forall t \in \mathcal{T} = \{1, \dots, n_t\}^3$:

$$\mathbf{c}_{p,t}^{\mathsf{fl}} + \lambda_{t}^{p} \mathbf{1}_{\mathsf{n}} - (\mathbf{M}_{\mathbf{p}_{t}}^{p_{t}^{\mathsf{l}}})_{\mathsf{n}}^{\mathsf{T}} \lambda_{t}^{p} - (\mathbf{M}_{\mathbf{p}_{t}}^{q_{t}^{\mathsf{l}}})_{\mathsf{n}}^{\mathsf{T}} \lambda_{t}^{q} + (\mathbf{M}_{\mathbf{p}_{t}}^{\underline{\mathbf{s}_{t}^{\mathsf{f}}}})_{\mathsf{n}}^{\mathsf{T}} \boldsymbol{\mu}_{s_{t}^{\mathsf{f}}} + (\mathbf{M}_{\mathbf{p}_{t}^{\mathsf{b}^{\mathsf{l}}}}^{\mathbf{s}_{t}^{\mathsf{l}}})^{\mathsf{T}} (\boldsymbol{\mu}_{\mathbf{v}_{t}^{\mathsf{l}}}^{-} - \boldsymbol{\mu}_{\mathbf{v}_{t}^{\mathsf{l}}}^{+}) + \boldsymbol{\mu}_{\mathbf{p}_{t}^{\mathsf{l}}}^{\mathsf{fl}} - \boldsymbol{\mu}_{\mathbf{p}_{t}^{\mathsf{l}}}^{\mathsf{fl}} - \boldsymbol{\mu}_{\mathbf{p}_{t}^{\mathsf{l}}}^{\mathsf{fl}} + (\mathbf{M}_{\mathbf{p}_{t}^{\mathsf{l}}}^{\mathbf{v}_{t}^{\mathsf{l}}})^{\mathsf{T}} (\boldsymbol{\mu}_{\mathbf{v}_{t}^{\mathsf{l}}}^{-} - \boldsymbol{\mu}_{\mathbf{v}_{t}^{\mathsf{l}}}^{+}) + \boldsymbol{\mu}_{\mathbf{p}_{t}^{\mathsf{l}}}^{\mathsf{fl}} - \boldsymbol{\mu}_{\mathbf{p}_{t}^{\mathsf{l}}}^{\mathsf{fl}} - \boldsymbol{\mu}_{\mathbf{p}_{t}^{\mathsf{l}}}^{\mathsf{fl}} - \boldsymbol{\mu}_{\mathbf{p}_{t}^{\mathsf{l}}}^{\mathsf{fl}} + (\mathbf{M}_{\mathbf{p}_{t}^{\mathsf{l}}}^{\mathbf{p}_{t}^{\mathsf{l}}})^{\mathsf{T}} (\boldsymbol{\mu}_{\mathbf{v}_{t}^{\mathsf{l}}}^{-} - \boldsymbol{\mu}_{\mathbf{v}_{t}^{\mathsf{l}}}^{\mathsf{fl}}) + \boldsymbol{\mu}_{\mathbf{p}_{t}^{\mathsf{l}}}^{\mathsf{fl}} - \boldsymbol{\mu}_{\mathbf{p}_{t}^{\mathsf{l}}}^{\mathsf{fl}} - \boldsymbol{\mu}_{\mathbf{p}_{t}^{\mathsf{l}}}^{\mathsf{fl}} - \boldsymbol{\mu}_{\mathbf{p}_{t}^{\mathsf{l}}}^{\mathsf{fl}} + (\mathbf{M}_{\mathbf{p}_{t}^{\mathsf{l}}}^{\mathbf{s}_{t}^{\mathsf{l}}})^{\mathsf{T}} \boldsymbol{\mu}_{\mathbf{s}_{t}^{\mathsf{l}}} + (\mathbf{M}_{\mathbf{p}_{t}^{\mathsf{l}}}^{\mathbf{s}_{t}^{\mathsf{l}}} + (\mathbf{M}_{\mathbf{p}_{t}^{\mathsf{l}}}^{\mathbf{s}_{t}^{\mathsf{l}}})^{\mathsf{T}} \boldsymbol{\mu}_{\mathbf{s}_{t}^{\mathsf{l}}} + (\mathbf{M}_{\mathbf{p}_{t}^{\mathsf{l}}}^{\mathbf{s}_{t}^{\mathsf{l}}})^{\mathsf{T}} \boldsymbol{\mu}_{\mathbf{s}_{t}^{\mathsf{l}}} + (\mathbf{M}_{\mathbf{p}_{t}^{\mathsf{l}}}^{\mathbf{s}_{t}^{\mathsf{l}}})^{\mathsf{T}} \boldsymbol{\mu}_{\mathbf{s}_{t}^{\mathsf{l}}} + (\mathbf{M}_{\mathbf{p}_{t}^{\mathsf{l}}}^{\mathbf{s}_{t}^{\mathsf{l}}} + (\mathbf{M}_{\mathbf{p}_{t}^{\mathsf{l}}}^{\mathbf{s}_{t}^{\mathsf{l}}})^{\mathsf{T}} \boldsymbol{\mu}_{\mathbf{s}_{t}^{\mathsf{l}}} + (\mathbf{M}_{\mathbf{p}_{t}^{\mathsf{l}}}^{\mathbf{s}_{t}^{\mathsf{l}}} + (\mathbf{M}_{\mathbf{p}_{t}^{\mathsf{l}}}^{\mathbf{s}_{t}^{\mathsf{l}}})^{\mathsf{T}} \boldsymbol{\mu}_{\mathbf{s}_{t}^{\mathsf{l}}} + (\mathbf{M}_{\mathbf{p}_{t}^{\mathsf{l}}}^{\mathbf{s}_{t}^{\mathsf{l}}})^{\mathsf{T}} \boldsymbol{\mu}_{\mathbf{s}_{t}^{\mathsf{l}}} + (\mathbf{M}_{\mathbf{p}_{t}^{\mathsf{l}}}^{\mathbf{s}_{t}^{\mathsf{l}}} + (\mathbf{M}_{\mathbf{p}_{t}^{\mathsf{l}}}^{\mathbf{s}_{t}^{\mathsf{l}}} + (\mathbf{M}_{\mathbf{p}_{t}^{\mathsf{l}}}^{\mathbf{s}_{t}^{\mathsf{l}}})^{\mathsf{T}} \boldsymbol{\mu}_{\mathbf{s}_{t}^{\mathsf{l}}} + (\mathbf{M}_{\mathbf{p}_{t}^{\mathsf{l}}}^{\mathbf{s}_{t}^{\mathsf{l}}})^{\mathsf{T}} \boldsymbol{\mu}_{\mathbf{s}_{t}^{\mathsf{l}}} + (\mathbf{M}_{\mathbf{p}_{t}^{\mathsf{l}}}^{\mathbf{s}_{t}^{\mathsf{l}}} + (\mathbf{M}_{\mathbf{p}_{t}^{\mathsf{l}}}^{\mathbf{s}_{t}^{\mathsf{l}}} + (\mathbf{M}_{\mathbf{p}_{t}^{\mathsf{l}}}^{\mathsf{l}} + (\mathbf{M}_{\mathbf{p}_{t}^{\mathsf{l}}}^{\mathsf{l}} + (\mathbf{M}_{\mathbf{p}_{t}^{\mathsf{l}}}^{\mathsf{l}} + (\mathbf{M}_{\mathbf{p}_{t}^{\mathsf{l$$

$$-\mathbf{M}_{\mathbf{p}_{t}}^{\underline{\mathbf{s}}_{t}^{\mathsf{T}}} \boldsymbol{\mu}_{s_{t}^{\mathsf{t}}} - \mathbf{M}_{\mathbf{p}_{t}}^{\mathbf{v}_{t}} \boldsymbol{\tau} (\boldsymbol{\mu}_{\mathbf{v}_{t}}^{-} - \boldsymbol{\mu}_{\mathbf{v}_{t}}^{+}) - \boldsymbol{\mu}_{\mathbf{p}_{t}}^{\mathsf{dg}+} + \boldsymbol{\mu}_{\mathbf{p}_{t}}^{\mathsf{dg}-} = 0, (20b)$$

$$\mathbf{c}_{q,t}^{\mathsf{g}} - \lambda_{t}^{q} \mathbf{1}_{\mathsf{N}} + \mathbf{M}_{\mathbf{q}_{t}}^{p_{t}^{\mathsf{T}}} \lambda_{t}^{p} + \mathbf{M}_{\mathbf{q}_{t}}^{q_{t}^{\mathsf{T}}} \lambda_{t}^{q} - \mathbf{M}_{\mathbf{q}_{t}}^{\underline{\mathbf{s}}_{t}^{\mathsf{T}}} \boldsymbol{\mu}_{s_{t}^{\mathsf{f}}}$$

$$\mathbf{c}_{q,t}^{\mathbf{c}} - \lambda_{\tilde{t}}^{\mathbf{t}} \mathbf{I}_{N} + \mathbf{M}_{\mathbf{q}_{t}}^{\mathbf{t}} \lambda_{\tilde{t}}^{\mathbf{t}} + \mathbf{M}_{\mathbf{q}_{t}}^{\mathbf{c}} \lambda_{\tilde{t}}^{\mathbf{t}} - \mathbf{M}_{\mathbf{q}_{t}}^{\mathbf{d}_{t}} \boldsymbol{\mu}_{s_{t}^{\mathbf{t}}}^{\mathbf{f}}$$
$$-\mathbf{M}_{\mathbf{q}_{t}}^{\mathbf{s}_{t}^{\mathbf{t}}} \boldsymbol{\mu}_{s_{t}^{\mathbf{t}}} - \mathbf{M}_{\mathbf{q}_{t}}^{\mathbf{v}_{t}\mathsf{T}} (\boldsymbol{\mu}_{\mathbf{v}_{t}}^{-} - \boldsymbol{\mu}_{\mathbf{v}_{t}}^{+}) - \boldsymbol{\mu}_{\mathbf{q}_{t}}^{\mathbf{d}g+} + \boldsymbol{\mu}_{\mathbf{q}_{t}}^{\mathbf{d}g-} = 0, \quad (20c)$$

$$-\mathbf{M}_{\mathbf{q}_{t}} \ \mu_{s_{t}^{t}} - \mathbf{M}_{\mathbf{q}_{t}} \ (\mu_{\mathbf{v}_{t}} - \mu_{\mathbf{v}_{t}}) - \mu_{\mathbf{q}_{t}} \ + \mu_{\mathbf{q}_{t}} = 0, (200)$$
$$-\lambda_{t}^{p} (\mathbf{1}_{\mathbf{N}}^{\mathsf{T}} \mathbf{p}_{t}^{g} - \mathbf{1}_{\mathbf{n}}^{\mathsf{T}} (\mathbf{p}_{t}^{cl} + \mathbf{p}_{t}^{g}) - \tilde{p}_{t}^{l}) = 0, \tag{20d}$$

$$-\lambda_t^q (\mathbf{1}_{\mathbf{N}}^{\mathsf{T}} \mathbf{q}_t^{\mathsf{g}} - \mathbf{1}_{\mathsf{n}}^{\mathsf{T}} (\mathbf{q}_t^{\mathsf{cl}} + \mathbf{q}_t^{\mathsf{fl}}) - \tilde{q}_t^{\mathsf{l}}) = 0, \tag{20e}$$

$$\boldsymbol{\mu}_{\mathbf{s}_{t}^{\mathrm{f}}}(|\underline{\tilde{\mathbf{s}}}_{t}^{\mathrm{f}}|^{2}-(\mathbf{s}_{t}^{\mathrm{f}+})^{2})=0,\ \boldsymbol{\mu}_{\mathbf{s}_{t}^{\mathrm{f}}}(|\underline{\tilde{\mathbf{s}}}_{t}^{\mathrm{t}}|^{2}-(\mathbf{s}_{t}^{\mathrm{t}+})^{2})=0, \tag{20f}$$

$$\boldsymbol{\mu}_{\mathbf{v}_{t}^{\mathrm{L}}}^{+}(\tilde{\mathbf{v}}_{t}^{\mathrm{L}}-\mathbf{v}_{t}^{L+})=0, \boldsymbol{\mu}_{\mathbf{v}_{t}^{\mathrm{L}}}^{-}(-\tilde{\mathbf{v}}_{t}^{\mathrm{L}}+\mathbf{v}_{t}^{L-})=0, \tag{20g}$$

$$\mu_{\mathbf{p}_{t}}^{\text{dg+}}(\mathbf{p}_{t}^{\text{dg}} - \mathbf{p}_{t}^{\text{dg+}}) = 0, \mu_{\mathbf{p}_{t}}^{\text{dg-}}(-\mathbf{p}_{t}^{\text{dg}} + \mathbf{p}_{t}^{\text{dg+}}) = 0, (20\text{h})$$

$$\mu_{\mathbf{q}_{t}}^{\text{dg+}}(\mathbf{q}_{t}^{\text{dg}} - \mathbf{q}_{t}^{\text{dg+}}) = 0, \mu_{\mathbf{q}_{t}}^{\text{dg-}}(-\mathbf{q}_{t}^{\text{dg}} + \mathbf{q}_{t}^{\text{dg+}}) = 0, (20\text{i})$$

$$\mu_{\mathbf{p}_{t}}^{\text{lf+}}(\mathbf{p}_{t}^{\text{lf}} - \mathbf{p}_{t}^{\text{lf+}}) = 0, \mu_{\mathbf{p}_{t}}^{\text{lf-}}(-\mathbf{p}_{t}^{\text{lf}} + \mathbf{p}_{t}^{\text{lf+}}) = 0, (20\text{j})$$

$$\mu_{\mathbf{p}_t}(\mathbf{p}_t - \mathbf{p}_t) = 0, \quad \mu_{\mathbf{p}_t}(-\mathbf{p}_t + \mathbf{p}_t) = 0, \quad (20\mathbf{j})$$

$$\mu_{\mathbf{p}_t}^{\text{fl}}(\mathbf{ch}_0^{\text{fl}} + \mathbf{D}_t \mathbf{p}_t^{\text{fl}} - \mathbf{z}_t - \mathbf{ch}_t^{\text{fl}}) = 0, \quad (20\mathbf{k})$$

$$\mu_{\mathbf{ch}_t}^{\mathrm{fl}-}(-\mathbf{ch}_0^{\mathrm{fl}} - \mathbf{D}_t \mathbf{p}_t^{\mathrm{fl}} + \mathbf{z}_t + \mathbf{ch}_t^{\mathrm{fl}-}) = 0, \tag{201}$$

along with all primal feasible conditions of the LMOPF and non-negative Lagrange multipliers.

For active powers, only stationary condition (20b) contains root-node, which due to the implicit definition (see Sec. IV-B) turns all the root-node entries in $\mathbf{M}^{[\cdot]}$ to zero, leading to

$$c_{p,t}^0 = -\lambda_t^p. (21)$$

Now let respective marginal values of DGs and FLs be,

$$\Pi_{\mathbf{p}_{t}^{\text{flex}}}^{\text{Flex}} := -\mathbf{c}_{p,t}^{\text{fl}} - \mu_{\mathbf{p}_{t}}^{\text{fl}+} + \mu_{\mathbf{p}_{t}}^{\text{fl}-} - \underbrace{\mathbf{D}_{t}(\mu_{\mathbf{ch}_{t}}^{\text{fl}+} - \mu_{\mathbf{ch}_{t}}^{\text{fl}-})}_{t} \in \mathbb{R}^{n}$$

$$\Pi_{\mathbf{p}_{t}^{\text{dg}}}^{\text{Flex}} := \mathbf{c}_{p,t}^{\text{dg}} + \mu_{\mathbf{p}_{t}}^{\text{dg}+} - \mu_{\mathbf{p}_{t}}^{\text{dg}-} \in \mathbb{R}^{n}$$
(22)

As the definitions in (22) represent internal constraints of the flexibility resources, the cleared DLMPs $\Pi_{\mathbf{p}_t}^{\text{Grid}}$, which is a grid equilibrium, must satisfy the following condition:

$$\Pi_{\mathbf{p}_{t}^{\text{flex}}}^{\text{Flex}} = \Pi_{\mathbf{p}_{t}}^{\text{Grid}} = \Pi_{\mathbf{p}_{t}^{\text{dg}}}^{\text{Flex}}.$$
 (23)

After substituting (21) in [(20a), (20b)] and then utilizing (23), we recover the individual components of $\Pi_{\mathbf{p}_t}^{\text{Grid}}$, as shown in (19). Moreover, from (23) these components exists in equilibrium. Hence, *Proposition 1* holds true.

Similar to active power DLMPs $\Pi_{\mathbf{p}_t}^{\text{Grid}}$, reactive power DLMPs $\Pi_{\mathbf{q}_t}^{\text{Grid}}$ can be derived using a similar method, i.e. evaluating the marginal cost of supplying reactive power at the root-node, $c_{a,t}^0$ with its corresponding stationary condition

 $^{^3}As$ stationary condition (20a) contains inter-temporal constraints, note that the last term only exists for non-terminal period, i.e., $\mathcal{T}\setminus|\mathcal{T}|$, else its zero [7]. Also in (20b), (20c) $\boldsymbol{\mu}_{\mathbf{v}_t}^{-/+}:=(0,\boldsymbol{\mu}_{\mathbf{v}_t^L}^{-/+\mathsf{T}})^\mathsf{T}$ as root-node voltage is fixed.

of (20c). However, whether this marginal cost of supplying reactive power at the root-node is made available by existing wholesale markets is still a topic of ongoing discussion [1], [17], [18]. Nevertheless, the presented model is flexible enough to provide an option of pricing reactive power only as a function of its marginal value at the root-node, i.e. $c_{q,t}^0$. If this information is not available at the root-node, this price can simply be set to zero.

E. DLMPs: Day-ahead Local Distribution Grid Market

We show in this subsection that the proposed DLMP model can be utilized by the DSO to operate a day-ahead local distribution grid market as:

- 1) The DSO forecasts its daily underlying grid demand along with the cost to supply it using the marginal-cost
- at the root-node, i.e. $c_{p,t}^0/c_{q,t}^0$; 2) DGs/FLs submit their day-ahead instantaneous/multitemporal bids, energy requirements and dispatch capabilities; and
- 3) The DSO clears DLMPs for each interval and pass them to DGs/FLs.

Now we show that this local market is able to achieve efficient flexible resource allocation. This means that the cleared DLMPs of the local market in (23), optimizing the overall system dispatch $\hat{\mathbf{s}}_t^{\text{disp}}$ in (15), achieves exactly same dispatch as to when DGs/FLs maximize their individual surpluses using their corresponding individual DLMPs. The following proposition shows this property.

Proposition 2: Under the assumption of no forecast error, the DSO cleared DLMPs $\Pi_{\mathbf{p}_t}^{\text{Grid}}$ correspond to a unique solution, maximizing the overall social welfare (15) as well as FLs' individual surplus⁴.

Proof: Consider individual FLs' maximization problem

$$\max \sum_{t \in T} -(\mathbf{\Pi}_{\mathbf{p}_{t}}^{\text{Grid}})^{\mathsf{T}} \mathbf{p}_{t}^{\mathsf{fl}}$$

$$\text{s.t.} \quad \mathbf{p}_{t}^{\mathsf{fl}-} \leq \mathbf{p}_{t}^{\mathsf{fl}} \leq \mathbf{p}_{t}^{\mathsf{fl}+} : \boldsymbol{\mu}_{\mathbf{p}_{t}}^{\mathsf{fl}-}, \boldsymbol{\mu}_{\mathbf{p}_{t}}^{\mathsf{fl}+}$$

$$\mathbf{ch}_{t}^{\mathsf{fl}-} \leq \mathbf{ch}_{0}^{\mathsf{fl}} + \mathbf{D}_{t} \mathbf{p}_{t}^{\mathsf{fl}} - \mathbf{z}_{t} \leq \mathbf{ch}_{t}^{\mathsf{fl}+} : \boldsymbol{\mu}_{\mathbf{ch}_{t}}^{\mathsf{fl}-}, \boldsymbol{\mu}_{\mathbf{ch}_{t}}^{\mathsf{fl}+}$$

$$(24a)$$

s.t.
$$\mathbf{p}_{t}^{\text{fl-}} \leq \mathbf{p}_{t}^{\text{fl}} \leq \mathbf{p}_{t}^{\text{fl+}} : \boldsymbol{\mu}_{\mathbf{p}_{t}}^{\text{fl-}}, \boldsymbol{\mu}_{\mathbf{p}_{t}}^{\text{fl+}}$$
 (24b)

$$\mathbf{ch}_t^{\mathsf{fl}-} \le \mathbf{ch}_0^{\mathsf{fl}} + \mathbf{D}_t \mathbf{p}_t^{\mathsf{fl}} - \mathbf{z}_t \le \mathbf{ch}_t^{\mathsf{fl}+} : \boldsymbol{\mu}_{\mathbf{ch}_t}^{\mathsf{fl}-}, \boldsymbol{\mu}_{\mathbf{ch}_t}^{\mathsf{fl}+} \quad (24c)$$

 $\forall t \in \mathcal{T} = \{1, \dots, n_t\}$. As LMOPF (15) has a strictly convex cost function (Remark 2), the inclusion of DLMPs (linear in $\mathbf{p}_{t}^{\text{fl}}$) also makes the cost function of individual FL problem (24a) strictly convex. Combining this with affine constraints (24b), (24c), the individual FLs problem (24) is then also a QP, with a unique minimizer $(\hat{\mathbf{p}}_t^{fl})^{ind}$ satisfying its following necessary and sufficient KKT conditions (25):

$$\Pi_{\mathbf{p}_{t}}^{\text{Grid}} + \mu_{\mathbf{p}_{t}}^{\text{fl+}} - \mu_{\mathbf{p}_{t}}^{\text{fl-}} + \underbrace{\mathbf{D}_{t}(\mu_{\mathbf{ch}_{t}}^{\text{fl+}} - \mu_{\mathbf{ch}_{t}}^{\text{fl-}})}_{\mathbf{D}_{t}(\mu_{\mathbf{ch}_{t}}^{\text{fl+}} - \mu_{\mathbf{ch}_{t}}^{\text{fl-}})} = 0,$$

$$\mu_{\mathbf{p}_{t}}^{\text{fl+}}(\mathbf{p}_{t}^{\text{fl}} - \mathbf{p}_{t}^{\text{fl+}}) = 0, \mu_{\mathbf{p}_{t}}^{\text{fl-}}(-\mathbf{p}_{t}^{\text{fl}} + \mathbf{p}_{t}^{\text{fl+}}) = 0,$$

$$\mu_{\mathbf{ch}_{t}}^{\text{fl+}}(\mathbf{ch}_{0}^{\text{fl}} + \mathbf{D}_{t}\mathbf{p}_{t}^{\text{fl}} - \mathbf{z}_{t} - \mathbf{ch}_{t}^{\text{fl+}}) = 0,$$

$$\mu_{\mathbf{ch}_{t}}^{\text{fl-}}(-\mathbf{ch}_{0}^{\text{fl}} - \mathbf{D}_{t}\mathbf{p}_{t}^{\text{fl}} + \mathbf{z}_{t} + \mathbf{ch}_{t}^{\text{fl-}}) = 0,$$
(25)

along with the primal feasible (24b), (24c) and all Lagrange multipliers non-negative constraints.

Observe that the grid cleared DLMPs, $\Pi_{\mathbf{p}_t}^{Grid}$, deployed in the individual problems of (25) are in equilibrium with

 $\Pi_{\mathbf{p}^{\text{flex}}}^{\text{Flex}}$ in (22). This makes all individual KKT conditions of (25), in fact, a part of the overall KKT conditions (20), meaning that a valid overall solution $(\hat{\mathbf{p}}_t^{\text{fl}})^{\text{all}}$, satisfying (20), is also a solution to (25). On the other hand, the individual problem (24) does not contain any grid constraints, so a valid individual solution ($\hat{\mathbf{p}}_t^{\text{fl}}$) ind to (25) may not necessarily satisfy (20). However, $\mathbf{\Pi}_{\mathbf{p}_t}^{\text{Grid}}$ shared among the individual and overall problem is obtained around a unique operating point, due to strictly convex subproblem (see Sec. IV-C3), making the overall solution $(\hat{\mathbf{p}}_t^{\text{fl}})^{\text{all}}$ of (20) unique. Moreover, as the individual FL problem (24) is also a strictly convex problem, it also constitutes a unique solution $(\hat{\mathbf{p}}_t^{fl})^{ind}$. Due to this uniqueness, both the individual problem solution and the overall solution are similar, i.e. $(\hat{\mathbf{p}}_t^{\mathrm{fl}})^{\mathrm{ind}} = (\hat{\mathbf{p}}_t^{\mathrm{fl}})^{\mathrm{all}}$.

F. Discussion

Practical Implication: The local distribution grid market proposal through the proposed method in Sec. IV-E can be simply extended to co-exist with the current wholesale dayahead energy markets [28]. This can be achieved by first FLs/DGs purchasing/selling energy from the wholesale market. The schedules of FLs/DGs are then submitted to the DSO. The DSO can then proceed to run its local market (steps 1-3 of Sec. IV-E) and formulate DLMPs, which are then passed on to FLs/DGs. FLs/DGs can then include these DLMPs into their individual energy planning and proceed with their participation in the day-ahead wholesale market.

Application Support: A possible application of the proposed day-ahead local market, described in Sec. IV-E, is in developing grid-friendly demand response and congestion management programs. This is possible because the cleared DLMP at a particular node (23) automatically reflects its contribution of delivered energy towards system losses, congestion and voltage violations. Hence, the submitted schedules by FLs/DGs can be evaluated by the DSO and eventually can lean towards more grid-friendly demand response and congestion management schemes. Note that for lossless DLMPs, similar model applications have been proposed in [5]-[8].

Formulation Extensions: Since the proposed model in (15) represents flexibility resources for both instantaneous and multi-period dispatch, this potentially allows for multiple formulation extensions. For example, multi-period FLs formulation in (15) can naturally be extended to include wide range of generic inter-temporal energy-constrained flexibility resources, such as energy storage systems and DGs with rampup/down limitations [1], [2].

V. SIMULATION SETUP & RESULTS

The proposed method is tested on the IEEE 33-bus distribution system [16]. The modified configuration of the grid is shown in Fig. 2. A realistic scenario with DGs and FLs operating under different cost functions and dispatch capabilities are simulated as follows; (1) the active and reactive power dispatch for DGs are within range [0, 0.5] MW and [-0.3, 0.3]MVar, with marginal cost of active and reactive power set at 10 \$/MWh and 3 \$/MVarh for the whole day and (2) the active power dispatch for FLs is within the range [-1.47, 0]MW (derived from [5]), to be optimized using the day-ahead cleared price at the root-node (taken from [5, Fig. 6]). A small

⁴Similar proposition and subsequent proof exists for DGs.

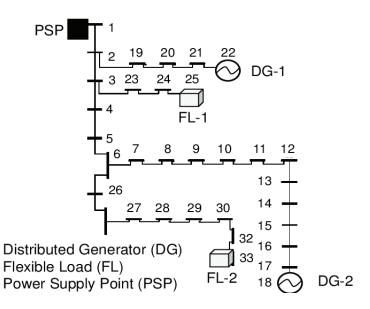


Fig. 2. The modified 33-bus distribution grid with two FLs and two DGs, with PSP (root-node) connection from the transmission grid. For fully exploring the proposed method FL-1 and DG-1 are placed closer to the root-node, whereas FL-2 and DG-2 are placed far from the root-node.

value of price sensitivity coefficient of 1e-4 \$/MWh²(MVarh²) is chosen to keep all cost functions strictly convex. This value is in line with the price sensitivity coefficients assumed in [7]⁵. More information on obtaining these coefficients is provided in [8], [9]. Parameters of the trust-region in Algorithm 1 are taken from [23]. All simulations are carried out on a 2.4-GHz processor with 64-GB RAM. Optimization problems are solved using YALMIP [29] with GUROBI [30] as a solver. Power flows for the trust-region evaluation steps in Algorithm 1 are performed using MATPOWER [21].

A. System Dispatch using DLMPs

To explore the proposed method in detail, we simulate three scenarios with the resultant active power DLMPs along with dispatch quantities presented in Fig. 3 and Fig. 4, respectively.

Scenario 1 is simulated by relaxing all nodal voltages and line flow constraints, i.e., to only show the effect of losses in DLMPs. As dispatching energy from DGs is cheaper than supplying from the root-node, i.e. 10 \$/MWh < $c_{p,t}^0$, $\forall t \in T$, they are fully dispatched for the whole time horizon in this scenario. However, this does not imply that nodes with DGs also experience lower DLMPs. This is because whenever DGs are dispatch fully, the extra MW amount comes from the higher marginal cost providing the root-node. At step 10, FLs draw a large amount of energy, raising their DLMP levels in proportion to their individual contributions towards the overall losses to the grid.

Scenario 2 constrains all nodal voltage magnitude between 0.92 and 1.05 p.u., causing an increase in DLMPs at time step 10 for FL2 as higher loading at node 33 binds lower voltage limits. As a consequence, FL2 draws lesser power at time step 10, as compared to Scenario 1. The same dispatch phenomenon is observed for DG1 (node 22), where active power dispatch reduces in order to adhere to its respective voltage limits. This causes DLMPs at node 22, now fully served by DG1 to be equal to its marginal cost, i.e., 10 \$/MWh, except at time step 10, where higher grid loading from FLs, allows DGs to dispatch fully, causing the extra MW amount to flow from the root-node and raising DLMP levels.

Scenario 3 constrains the distribution line serving FL1 by 1.6 MVA. As compared to Scenario 1 & 2, this reduces the power drawn by FL1 at time step 10 and increases its DLMP value due to binding line flows.

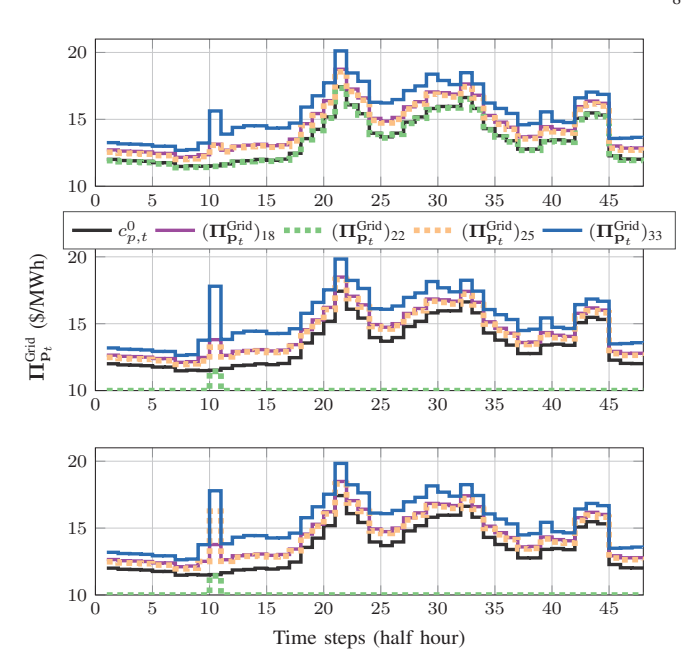


Fig. 3. Active power DLMPs for *Scenario* 1 (top), 2 (middle) and 3 (bottom) for all flexible nodes along with the marginal cost at the root-node $c_{p,t}^0$.

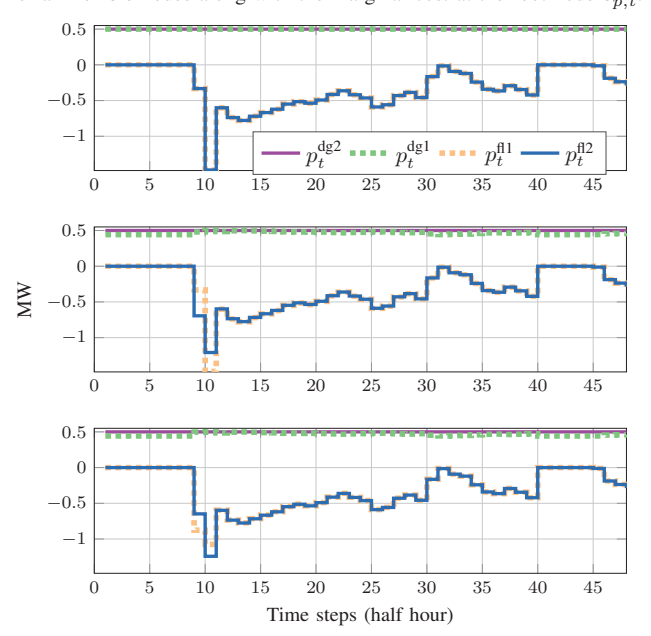


Fig. 4. Active power dispatch values for *Scenario* 1 (top), 2 (middle) and 3 (bottom) for all flexible nodes.

For time step 10 and all scenarios, we present market equilibrium in Table 1. In Table 1, $\Pi^{\rm M}_{{\bf p}_t}=\mu^{{\rm fl}+/{\rm dg}+}_{{\bf p}_t}-\mu^{{\rm fl}-/{\rm dg}-}_{{\bf p}_t}$, and $\Pi^{\rm D}_{{\bf p}_t}={\bf D}_t(\mu^{{\rm fl}+}_{{\bf ch}_t}-\mu^{{\rm fl}-}_{{\bf ch}_t})$. Shown in bold in Table 1, it can be observed that flexible DLMPs representing the internal flexible node dynamics exist in equilibrium with the grid cleared DLMPs, i.e., $\Pi^{\rm Grid}_{{\bf p}_t}=\Pi^{\rm Flex}_{{\bf p}_t^{\rm dg/fl}}$.

B. Model Comparisons

In Fig. 5, the performance of the proposed LMOPF model is compared against a state-of-the-art linearized power flow model (LIOPF) [10] and an interior point MATPOWER model (ACOPF) [21]. As LIOPF and MATPOWER only provide DLMPs for a single time step (instantaneous dispatch),

⁵A considerably large value of these coefficients makes flexible resources to dispatch their schedule more conservatively, as then the quadratic term (Hessian) dominates their respective cost functions (see *Definition* 1).

TABLE I DLMPs for scenario 1 (top), 2 (middle) and 3 (bottom) at time step t=10 and node i.

i	$\mathbf{\Pi}_{\mathbf{p}_t}^{\mathrm{E}}$	$\Pi^{ ext{L}}_{\mathbf{p}_t}$	$\Pi^{\mathrm{C}}_{\mathbf{p}_t}$	$\Pi^{\mathbb{V}}_{\mathbf{p}_t}$	$\mathbf{\Pi}^{ ext{Grid}}_{\mathbf{p}_t}$	$\mathbf{c}_{p,t}^{\mathrm{dg/fl}}$	$\mathbf{\Pi}_{\mathbf{p}_t}^{\mathrm{M}}$	$\Pi^{\mathrm{D}}_{\mathbf{p}_t}$	$\mathbf{\Pi}^{\mathrm{Flex}}_{\mathbf{p}^{\mathrm{dg}/\mathrm{f}}_t}$
18 22 25 33	11.52	1.62 -0.04 1.53 4.10	0 0 0 0	0 0 0 0	13.14 11.48 13.06 15.63	10 -11.52	3.14 1.48 -2.84 -1.41	- 27.42 28.56	13.14 11.48 13.06 15.63
18 22 25 33	11.52	1.45 -0.04 1.48 3.50	0 0 0 0	0.83 -0.04 0.24 2.78	13.80 11.44 13.25 17.80	10 -11.52	3.80 1.44 -2.67 0	- 27.44 29.32	13.80 11.44 13.25 17.80
18 22 25 33	11.52	1.42 -0.05 1.26 3.50	0 0 0.23 0	0.82 -0.04 3.25 2.76	13.77 11.42 16.26 17.79	10 -11.52	3.77 1.42 0 0	- 27.79 29.32	13.77 11.42 16.26 17.79

we also adopt our proposed model for single time step. The dispatch capabilities of DGs/FLs remain the same as during the previous scenarios, however we simulate two cases to fully explore the proposed model.

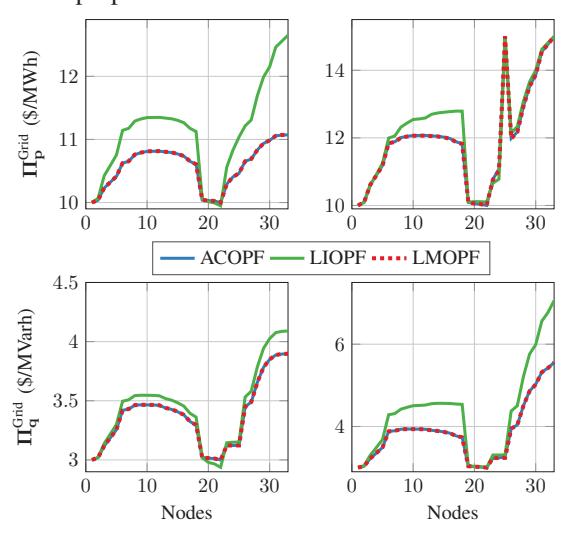


Fig. 5. Active (top) and reactive power (bottom) DLMPs of ACOPF [21], LIOPF [10] and the proposed LMOPF methods for *case-1* (left) and *case-2* (right).

Case-1: For all flexible nodes and the root-node, this case fixes the active and reactive power marginal costs at 10 \$/MWh and 3 \$/MVarh. It can be observed in Table 2 that the proposed LMOPF method achieves almost identical dispatch quantities and DLMPs to the non-convex ACOPF solution. Moreover, the proposed LMOPF, utilizing trust-region iterations, provides an improved solution quality compared to the LIOPF method. This is because for nodes far from the root-node large voltage drops exist causing higher errors in linearization, which is performed around a flat nodal voltage profile (1 p.u) and negligible angle difference. As FLs, due to their locations, with same marginal values to DGs are not dispatched, next we present Case-2 to evaluate their presence on DLMPs.

Case-2: In this case, marginal utility for all FLs are increased to 15 \$/MWh, all remaining settings are similar to Case-1. The proposed LMOPF method again achieves almost identical dispatch quantities and DLMPs as compared to the non-convex ACOPF solution [21]. The large power drawn by

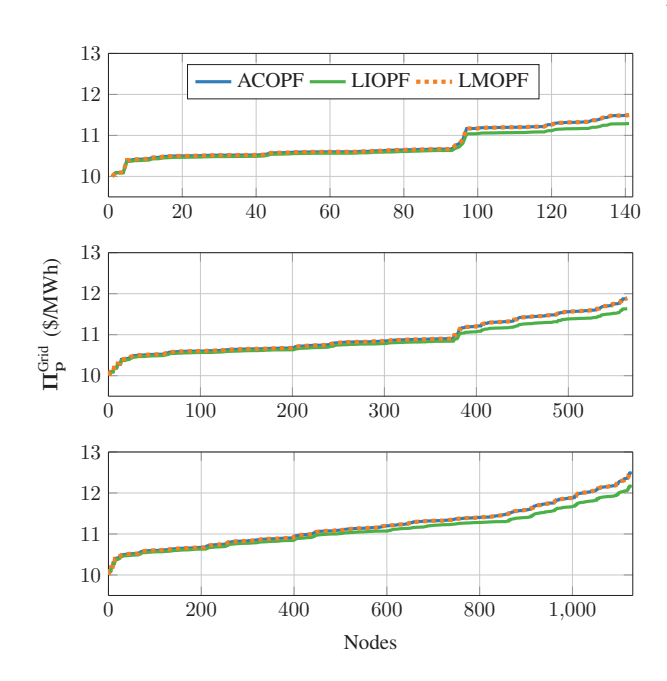


Fig. 6. Active power DLMP comparison between the proposed LMOPF, ACOPF [21] and LIOPF [10] for 141-nodes (top), 564-nodes (middle) and 1128-nodes (bottom) grid.

the FLs now binds the lower voltage and line flow limit at node 25 and 33.

TABLE II DISPATCH QUANTITY COMPARISON

	Units -	Case-1			Case-2			
	Omts -	ACOPF	LMOPF	LIOPF	ACOPF	LMOPF	LIOPF	
DG1	MW	0.50	0.50	0.50	0.50	0.50	0.50	
	MVar	0.30	0.30	0.30	0.30	0.30	0.30	
DCO	MW	0.28	0.29	0	0.39	0.39	0.50	
DG2	MVar	0.13	0.13	0	0.12	0.12	0.17	
FL1	MW	0	0	0	-1.16	-1.10	-1.09	
FL2	MW	0	0	0	-1.24	-1.25	-1.36	

The general observation from both cases is that for nodes 19-22, similar DLMPs are obtained from all three methods. This happens because voltage magnitudes are close to their upper voltage limits and binding at node 22, making its feed-in branch experiencing DLMPs at its marginal cost, i.e. 10 \$/MWh and 3 \$/MVarh. For Case-2, this effect is also caused by line flow constraint binding at node 33, causing the respective DLMPs to be closer to FLs' marginal utility value, i.e. 15 \$/MWh. It was also confirmed that, for both cases, regardless of the initialization point, the proposed LMOPF method always converged to the same dispatch and consequently DLMPs (solution uniqueness) within only 4 iterations.

C. Model Scalability

To show the effectiveness of the proposed model, we implement the proposed model on three distribution grids containing 141-nodes [31], 564-nodes and 1128-nodes. For all the grids, the marginal cost settings for DGs/FLs are kept similar to those of *Case-2* of Sec. V-B. We make the 564-nodes and the 1128-nodes grid by duplicating the 141-nodes grid, while

preserving its original root-node [10]. Similarly, the number of DGs/FLs in the 564-nodes grid and the 1128-nodes grid are proportionally increased as compared to 141-nodes grid. In this way, we not only evaluate the feasible solution projection step but also the trust-region minimization step of the proposed model (See Algorithm 1).

The comparison of the proposed model with other methods in the literature is also shown in Fig. 6. We only present active power DLMPs in Fig. 6 as reactive power DLMPs show similar results and are left out here to save space. Similar to Fig. 5, Fig. 6 reiterates that the proposed model achieves the same results as MATPOWER's interior point ACOPF model, while outperforming the state-of-the-art linearized model [10]. It is to be noted that both the interior point and semidefinite programming ACOPF solvers of MATPOWER produced exactly the same result. Table. III details the information regarding the simulated grids and the resultant computation efforts of the proposed model. It can be seen that the proposed model scales well with the increase in the size of the grid and the number of flexibility resources (DGs/FLs).

PROPOSED MODEL SCALABILITY

Nodes	DGs	FLs	Iteration	Time (sec.)
141	2	2	3	1.5
564	8	8	3	3.3
1128	16	16	4	13.3

VI. CONCLUSION & FUTURE WORKS

We proposed a new distribution locational marginal price (DLMP) model which utilized the classical global energy balance formulation and combined with the recent works on AC power flow linearization. Relevant for DLMPs, we extended the AC power flow linearizations to represent grid losses and line flows. The developed model showed that it is able to depict market equilibrium conditions and efficiently allocates flexible resources in a day-ahead local market. Moreover the calculated DLMPs are decomposable into their most generic grid components of energy, loss, congestion and voltage. To show the efficacy of the proposed model, we implemented on a benchmark distribution systems and compared it with other state-of-the-art methods.

An interesting future works exists in extending the proposed model to include various energy storage systems and DGs with ramp-up/down limitations; generic multiphase and unbalanced distribution grids; and voltage, current and impedance dependent load models.

VII. APPENDIX

A. Cost/Utility Functions

Let λ be the cleared active power per unit price, then the cost/utility function for DGs/FLs in (1) follows:

$$\begin{split} \mathbf{p}_{t}^{\text{fl}} &= \underset{\mathbf{p}_{t}^{\text{fl}} \in \mathbb{R}^{\text{n}}}{\operatorname{argmax}} \ \mathbf{U}_{t}^{\text{fl}}(\mathbf{p}_{t}^{\text{fl}}) - \lambda \mathbf{p}_{t}^{\text{fl}} = \max \left\{ 0, \left\{ \mathbf{p}_{t}^{\text{fl}} \mid \frac{\partial \mathbf{U}_{t}^{\text{fl}}(\mathbf{p}_{t}^{\text{fl}})}{\partial \mathbf{p}_{t}^{\text{fl}}} = \lambda \right\} \right\}, \\ \mathbf{p}_{t}^{\text{g}} &= \underset{\mathbf{p}_{t}^{\text{g}} \in \mathbb{R}^{\text{n}}}{\operatorname{argmax}} \ \lambda \mathbf{p}_{t}^{\text{g}} - \mathbf{C}_{t}^{\text{g}}(\mathbf{p}_{t}^{\text{g}}) = \max \left\{ 0, \left\{ \mathbf{p}_{t}^{\text{g}} \mid \frac{\partial \mathbf{C}_{t}^{\text{g}}\left(\mathbf{p}_{t}^{\text{g}}\right)}{\partial \mathbf{p}_{t}^{\text{g}}} = \lambda \right\} \right\}. \end{split}$$

Same interpretation holds for reactive power cost functions.

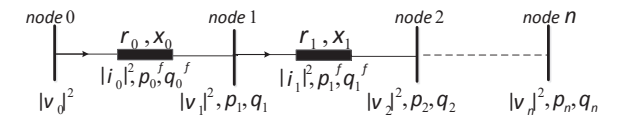


Fig. 7. Notations used to represent branch flow convexified power flow model of the radial grid [26]. For line connecting node j and k, squared line current, active power flow, reactive power flow, resistance and reactance are represented as: $i_j^{sq} := |i_j|^2$, p_j^f , q_j^f , r_j and x_j , respectively. For node j, squared voltage, active power injection and reactive power injection are represented as: $v_j^{sq} := |v_j|^2$, p_j and q_j , respectively.

B. Convexified DLMP Formulation

In order to aid in developing branch flow convexification method [16], [26], [27], we adopt scalar notation here to represent a radial grid in Fig. 7. We formulate convexified ACOPF for a generic injections (p_j, q_j) at each node jand single time-step in (26)⁶. In (26), s_j^f and $c_j^p(\cdot)/c_j^q(\cdot)$ are respectively the scalar version of the line flow "from" and cost function given in (7) and Sec. VII-A. For more information regarding the formulation, interested readers are referred to [26]. Constraints (26b)-(26e) represent AC power flow relaxation. The constraint (26e) is actually a second order cone constraint, if satisfied as an equality constraint makes the relaxation exact [27]. For detailed information on SOCP, interested readers are referred to [26], [27].

$$\max -\sum_{j=1}^{n} \left(c_{j}^{p}(p_{j}) + c_{j}^{q}(q_{j}) \right)$$
 (26a)

s.t.

$$p_j^f = p_{j+1}^f + r_j i_j^{sq} - p_{j+1} \qquad \qquad : \lambda_j^p \qquad (26b)$$

$$q_i^f = q_{i+1}^f + x_j i_i^{sq} - q_{j+1}$$
 : λ_i^q (26c)

$$v_j^{sq} = v_{j+1}^{sq} + 2(r_j p_j^f + x_j q_i^f) - (r_j^2 + x_j^2) i_j^{sq} : \lambda_j^v$$
 (26d)

$$\frac{(p_j^f)^2 + (q_j^f)^2}{v_j^{sq}} \le i_j^{sq} \qquad : \mu_j^i \qquad (26e)$$

$$(p_j^f)^2 + (q_j^f)^2 \le (s_j^{f+})^2$$
 : μ_j^s (26f)

$$v_{j}^{sq-} \leq v_{j}^{sq} \leq v_{j}^{sq+} \qquad : \mu_{j}^{v-}, \mu_{j}^{v+}$$

$$\forall j \in \{0, \dots, n-1\}$$
(26g)

Now considering an exact solution of (26), the following KKT conditions are then satisfied:

$$c_i^p + \lambda_i^p = 0 (27a)$$

$$c_i^q + \lambda_i^q = 0 \tag{27b}$$

$$\lambda_{i-1}^{p} = \lambda_{i}^{p} + 2r_{j}\lambda_{i}^{v} - 2p_{i}^{f}(\beta_{j} + \mu_{i}^{s}) = 0$$
 (27c)

$$\lambda_{j-1}^q = \lambda_j^q + 2x_j \lambda_j^v - 2q_j^f(\beta_j + \mu_j^s) = 0$$
 (27d)

$$r_j \lambda_j^p + x_j \lambda_j^q - (r_j^2 + x_j^2) + \mu_j^i = 0$$
 (27e)

$$\mu_{j}^{i} \frac{(p_{j}^{f})^{2} + (q_{j}^{f})^{2}}{(v_{j}^{sq})^{2}} + \mu_{j}^{v+} - \mu_{j}^{v-} + \lambda_{j}^{v} - \lambda_{j-1}^{v} = 0$$
 (27f)
$$\forall j \in \{1, \dots, n\}$$

Along with the primal feasible (26) and non-negative Lagrange multipliers conditions. In (27), we have $\beta_j := \frac{\mu_j^i}{v_j^{sq}}$.

⁶The full formulation (analogous to (9)) which considers FLs/DGs along with inter-temporal energy and actuator constraints is a straight forward procedure and is left out here for exposition simplicity and brevity.

For active power, consider DLMP at node j to be defined as λ_j^p . Then from (27c), we have DLMP at node (j) λ_j^p dependent upon DLMP at its ancestor-node (j-1) λ_{j-1}^p , along with other terms which are only dependent on the node (j) $2r_j\lambda_j^v$ and the line connecting the node (j) and its ancestor-node (j-1) $2p_j^f(\beta_j+\mu_j^s)$. Same explanation holds for the reactive power DLMP at node (j), i.e., λ_j^q .

1) DLMP Representation Issues: The DLMP value obtained from the above mentioned convexified formulation (27) might be interpreted as follows: a marginal change in injection at node (j) only requires a marginal change of injections at its own node (j) and its ancestor-node (j-1), while leaving reset of the grid unaffected. However, this interpretation is not physically true. As it has been shown in [3, Proposition 3.3] that a marginal change in the injection at node j also affects variables (e.g. voltages, line flows) at nodes other than its ancestor-node (j-1). Moreover, Lagrange multipliers λ_j^v and μ_j^i do not have straight forward interpretation. In light of these representation issues, we adopt global power balance formulation and its trust-region based iterative linearization for calculating DLMPs.

REFERENCES

- [1] M. Caramanis, E. Ntakou, W. W. Hogan, A. Chakrabortty, and J. Schoene, "Co-optimization of power and reserves in dynamic T&D power markets with nondispatchable renewable generation and distributed energy resources," *Proceedings of the IEEE*, vol. 104, no. 4, pp. 807–836, 2016.
- [2] G. T. Heydt, B. H. Chowdhury, M. L. Crow, D. Haughton, B. D. Kiefer, F. Meng, and B. R. Sathyanarayana, "Pricing and control in the next generation power distribution system," *IEEE Transactions on Smart Grid*, vol. 3, no. 2, pp. 907–914, 2012.
- [3] A. Papavasiliou, "Analysis of distribution locational marginal prices," IEEE Transactions on Smart Grid, 2017.
- [4] F. C. Schweppe, M. C. Caramanis, R. D. Tabors, and R. E. Bohn, Spot Pricing of Electricity, ser. The Kluwer International Series in Engineering and Computer Science, Power Electronics & Power Systems. Boston, MA: Springer US, 1988.
- [5] S. Hanif, T. Massier, H. B. Gooi, T. Hamacher, and T. Reindl, "Cost optimal integration of flexible buildings in congested distribution grids," *IEEE Transactions on Power Systems*, 2016.
- [6] S. Hanif, H. B. Gooi, T. Massier, T. Hamacher, and T. Reindl, "Distributed congestion management of distribution grids under robust flexible buildings operations," *IEEE Transactions on Power Systems*, p. 1, 2017.
- [7] R. Li, Q. Wu, and S. S. Oren, "Distribution locational marginal pricing for optimal electric vehicle charging management," *IEEE Transactions* on *Power Systems*, vol. 29, no. 1, pp. 203–211, 2014.
- [8] S. Huang, Q. Wu, S. S. Oren, R. Li, and Z. Liu, "Distribution locational marginal pricing through quadratic programming for congestion management in distribution networks," *IEEE Transactions on Power Systems*, vol. 30, no. 4, pp. 2170–2178, 2015.
- [9] R. A. Verzijlbergh, L. J. de Vries, and Z. Lukszo, "Renewable energy sources and responsive demand. do we need congestion management in the distribution grid?" *IEEE Transactions on Power Systems*, vol. 29, no. 5, pp. 2119–2128, 2014.
- [10] H. Yuan, F. Li, Y. Wei, and J. Zhu, "Novel linearized power flow and linearized opf models for active distribution networks with application in distribution lmp," *IEEE Transactions on Smart Grid*, p. 1, 2016.
- [11] L. Bai, J. Wang, C. Wang, C. Chen, and F. F. Li, "Distribution locational marginal pricing (dlmp) for congestion management and voltage support," *IEEE Transactions on Power Systems*, vol. PP, no. 99, pp. 1–1, 2017.
- pp. 1–1, 2017.
 [12] Z. Yuan, M. R. Hesamzadeh, and D. Biggar, "Distribution locational marginal pricing by convexified acopf and hierarchical dispatch," *IEEE Transactions on Smart Grid*, vol. PP, no. 99, pp. 1–1, 2016.
- [13] P. M. Sotkiewicz and J. M. Vignolo, "Nodal pricing for distribution networks: efficient pricing for efficiency enhancing dg," *IEEE Transactions* on *Power Systems*, vol. 21, no. 2, pp. 1013–1014, May 2006.
- on Power Systems, vol. 21, no. 2, pp. 1013–1014, May 2006.
 [14] S. Bolognani and S. Zampieri, "On the existence and linear approximation of the power flow solution in power distribution networks," *IEEE Transactions on Power Systems*, vol. 31, no. 1, pp. 163–172, Jan. 2016.

- [15] A. Conn, N. Gould, and P. Toint, Trust Region Methods. Society for Industrial and Applied Mathematics, 2000.
- [16] M. Baran and F. F. Wu, "Optimal sizing of capacitors placed on a radial distribution system," *IEEE Transactions on Power Delivery*, vol. 4, no. 1, pp. 735–743, 1989.
- [17] J. B. Gil, T. G. S. Roman, J. J. A. Rios, and P. S. Martin, "Reactive power pricing: a conceptual framework for remuneration and charging procedures," *IEEE Transactions on Power Systems*, vol. 15, no. 2, pp. 483–489, May 2000.
- [18] J. Zhong and K. Bhattacharya, "Toward a competitive market for reactive power," *IEEE Transactions on Power Systems*, vol. 17, no. 4, pp. 1206– 1215, Nov 2002.
- [19] N. Hatziargyriou, Microgrid: Architecture and Control. Wiley, 2014.
- [20] S. Bolognani and F. Dörfler, "Fast power system analysis via implicit linearization of the power flow manifold," in *Proc. 53rd Annual Allerton Conference on Communication, Control, and Computing*, 2015.
- [21] D. Z. Ray, E. M. S. Carlos, and J. T. Robert, "Matpower: Steady-state operations, planning, and analysis tools for power systems research and education," *IEEE Transactions on Power Systems*, vol. 26, no. 1, pp. 12–19, 2011.
- [22] W. H. Kersting, Distribution System Modeling and Analysis, Third Edition. Boca Raton: CRC Press, 2012.
- [23] A. M. Giacomoni and B. F. Wollenberg, "Linear programming optimal power flow utilizing a trust region method," in *North American Power* Symposium 2010, Sept 2010, pp. 1–6.
- [24] J. Lavaei, D. Tse, and B. Zhang, "Geometry of power flows and optimization in distribution networks," *IEEE Transactions on Power Systems*, vol. 29, no. 2, pp. 572–583, March 2014.
- [25] B. Zhang, A. Y. S. Lam, A. D. Domnguez-Garca, and D. Tse, "An optimal and distributed method for voltage regulation in power distribution systems," *IEEE Transactions on Power Systems*, vol. 30, no. 4, pp. 1714–1726, July 2015.
- [26] N. Li, L. Chen, and S. H. Low, "Exact convex relaxation of opf for radial networks using branch flow model," in 2012 IEEE Third International Conference on Smart Grid Communications (SmartGridComm), Nov 2012, pp. 7–12.
- [27] M. Farivar and S. H. Low, "Branch flow model: Relaxations and convexification-part i," *IEEE Transactions on Power Systems*, vol. 28, no. 3, pp. 2554–2564, Aug 2013.
- [28] Pennsylvania, Jersey, Maryland Power Pool (PJM), "Overview of the energy market: Pjm," 2017. [Online]. Available: https://tinyurl.com/ya4semfa
- [29] J. Löfberg, "Yalmip: A toolbox for modeling and optimization in MATLAB," in *Proceedings of the CACSD Conference*, Taipei, Taiwan, 2004
- [30] I. Gurobi Optimization, "Gurobi optimizer reference manual," 2016. [Online]. Available: http://www.gurobi.com
- [31] H. Khodr, F. Olsina, P. D. O.-D. Jesus, and J. Yusta, "Maximum savings approach for location and sizing of capacitors in distribution systems," *Electric Power Systems Research*, vol. 78, no. 7, pp. 1192 – 1203, 2008.



Sarmad Hanif (S'15) received B.Sc. in Electrical Engineering from the University of Engineering and Technology Lahore, Pakistan and M.Sc. in Power Engineering from the Technical University of Munich (TUM), Germany in 2009 and 2013, respectively. Since June 2014, he is pursuing Ph.D. at the Technical University of Munich (TUM), Germany. He is interested in applications of optimization and microeconomics in power systems.



Kai Zhang (S'16) received his B.Sc. degree in electrical and electronic engineering from University of Duisburg-Essen (UDE) in 2013 and M.Sc. degree in electrical engineering and information technology from Technical University of Munich (TUM) in 2016. Since August 2016, he is working as research associate at TUMCREATE in Singapore and pursuing his PhD. His research interests include large-scale power system optimization using distributed techniques and online optimization algorithms.



Christoph M. Hackl (M'12-SM'16) was born in 1977 in Mannheim, Germany. After studying electrical engineering (controls and mechatronics) at Technical University of Munich (TUM, Germany) and University of Wisconsin-Madison (USA), he received the B.Sc., Dipl.-Ing., and Dr.-Ing. (Ph.D.) degree in 2003, 2004 and 2012 from TUM, respectively. Since 2004, he is teaching electrical drives, power electronics, and mechatronic & renewable energy systems. Since 2014, he is heading the research group "Control of Renewable Energy Sys-

tems (CRES)" at TUM. In 2018, he was appointed Professor for Electrical Machines and Drives at the Munich University of Applied Sciences (MUAS), Germany. His main research interests are nonlinear, adaptive and optimal control of electric, mechatronic and renewable energy systems.



Masoud Barati (SM'18) received the Ph.D. degree in electrical engineering from Illinois Institute of Technology, Chicago, in 2013. Presently, he is an assistant professor in the Electrical and Computer Engineering Department at Louisiana State University, Baton Rouge, USA. His research interests include optimization, microgrid operation and planning, microeconomics, mathematical modeling and multiple infrastructure assessment.



H. B. Gooi (SM'95) received the B.S. degree in EE from National Taiwan University in 1978; the M.S. degree in EE from the University of New Brunswick in 1980; and the Ph.D. degree in EE from Ohio State University in 1983. From 1983 to 1985, he was an Assistant Professor with Lafayette College, Easton. From 1985 to 1991, he was a Senior Engineer with Empros (now Siemens), Minneapolis, where he was responsible for the design and testing coordination of domestic and international energy management system projects. In 1991, he joined the School of

Electrical and Electronic Engineering, Nanyang Technological University, Singapore, as a Senior Lecturer, where he has been an Associate Professor since 1999. He was the Deputy Head of Power Engineering Division during 2008-2014. He has been an Editor of IEEE Transactions on Power Systems since 2016. His current research interests include microgrid energy management systems dealing with storage, renewable energy sources, electricity market and spinning reserve.



Thomas Hamacher is a full professor in renewable and sustainable energy systems at the Technical University Munich (TUM), Germany. His research focuses on energy and systems analysis, focusing on urban energy systems, the integration of renewable energy into the power grid, and innovative nuclear systems (including fusion). Other focuses of his work are the methods and fundamentals of energy models.